Effect of Photoreduction Process on Self-cleaning and Antibacterial Activity of Au-doped TiO_2 Colloids on Cotton Fabric

Esfandiar Pakdel [a], Walid A. Daoud [b], Xungai Wang [a] *

[a] *The Hong Kong Polytechnic University, School of Fashion and Textiles, Research Centre of Textiles for Future Fashion, JC STEM Lab of Sustainable Fibers and Textiles, Hung Hom, Kowloon, Hong Kong*

[b] *Department of Mechanical Engineering, City University of Hong Kong, Hong Kong*

Corresponding author:

Prof. Xungai Wang (Email: xungai.wang@polyu.edu.hk),

Tel: (+852) 2766 6437

Abstract

This study aims at understanding the effect of photoreduction process during the synthesis of gold (Au)-doped TiO_2 colloids on the conferred functionalities on cotton fabrics. TiO_2/Au and TiO_2/Au/SiO_2 colloids were synthesised through the sol-gel method with and without undergoing the photoreduction step based on different molar ratios of Au:Ti (0.001 and 0.01) and TiO_2/SiO_2 (1:1 and 1:2.3). The colloids were applied to cotton fabrics and the obtained photocatalytic self-cleaning, wet photocatalytic activity, UV protection, and antibacterial activity against *E. coli* and *S. aureus* bacteria were investigated. The obtained results demonstrated that the photoreduction of Au weakened the self-cleaning effect and reduced the photocatalytic activity of coated fabrics. Also, an excess amount of Au deteriorated the photocatalytic activity under both UV and visible light. The most efficient self-cleaning effect was obtained on fabrics coated with ternary TiO_2/Au/SiO_2 colloid containing ionic Au where it decomposed coffee and red-wine stains after 3h of illumination. Adding silica (SiO_2) made the fabrics superhydrophilic and led to a greater methylene blue (MB) dye adsorption, faster dye degradation pace, and more-efficient stain removal. Moreover, the photoreduction process affected Au nanoparticles (NPs) size, weakened the antibacterial activity of fabrics against both types of tested bacteria, while modestly increased the UV-protection. In general, the photoactivity of Au-doped colloids was influenced by the synthesis method, ionic and metallic state of Au dopant, the concentration of Au dopant, and the presence and concentration of silica.

Keywords: Photocatalyst, Self-cleaning, TiO_2, Antibacterial textiles, UV protection

1. Introduction

The implementation of the self-cleaning technology in textiles has been realised based on two main mechanisms including superhydrophobic coatings [1] and photocatalytic nanocoatings [2]. For the latter mechanism, a thin layer of photocatalytic nanomaterials such as titanium dioxide (TiO_2) [3], zinc oxide (ZnO) [4], and graphitic carbon nitride nanosheets (g-C_3N_4) [5] is applied to a textile substrate and then immobilised via different techniques. The photocatalytic nature of the nanocoatings breaks down the adsorbed organic contaminants such as stains and microorganisms into harmless products under light irradiation [6]. For this type of nanocoatings, hydrophilicity is an advantage as it can boost the photocatalytic activity which results in an enhanced self-cleaning property [7, 8]. Among different types of photocatalysts, TiO_2 has widely been used in surface functionalisation of textiles through different methods such as sol-gel, sonication, hydrothermal, and cross-linking on various types of fabrics including cotton, wool, polyester, cashmere, and silk, among others [9]. Despite having numerous advantages such as abundance, low-cost, photostability, and non-toxicity, TiO_2 has some intrinsic disadvantages which have limited its applications [10, 11]. For instance, pure TiO_2 can only harness the energy of ultraviolet (UV) light, which accounts for around 4% of the solar spectrum, due to its wide band gap [3, 10]. TiO_2 can absorb incident light with energy equal or greater than its band gap (3.2 eV for anatase TiO_2) leading to the excitation of electrons from the valence band (VB) to the conduction band (CB) [12]. This process generates pairs of electrons (e^-) and holes (h^+) which can react with oxygen and water molecules producing superoxide anions ($O_2^{\cdot-}$) and hydroxyl radicals (OH·), respectively [13]. These reactive species react with organic compounds, breaking them down to nontoxic or colourless products such as water and carbon dioxide molecules [13, 14]. Rapid recombination of generated electrons and holes is another drawback of TiO_2 which results in a low photocatalytic yield [15]. Therefore, several factors such as particle size, bandgap,

crystallinity, surface area, interface characteristics, and the rate of recombination of electron-hole pairs determine the overall photocatalytic activity of TiO_2 NPs [3, 11].

Different methods such as doping with metals and non-metals, ion-doping, dye sensitisation, and coupling of semiconductors have been used to enhance the photocatalytic activity of TiO_2 and shift its activation threshold to the visible-light region [11, 15]. These methods are efficient based on different mechanisms. For instance, through modifying TiO_2 with noble metals such as gold (Au) and silver (Ag), the photocatalytic activity can be enhanced through reducing the recombination of photogenerated electron-hole pairs, and providing a surface plasmon resonance (SPR) effect [10]. To this end, various methods such as sol-gel, hydrothermal/solvothermal, impregnation, ion exchange, and photoreduction (photo-deposition), have been used to synthesise modified TiO_2 NPs[16, 17]. Of these methods, the photoreduction process, which is carried out under UV irradiation, has frequently been used, mostly because of its convenient use at room temperature, high efficiency, not involving chemicals, and uniform distribution of metal dopants in the supporting matrix [16, 18]. During the illumination process, light-induced electrons from TiO_2 can react with metal precursors forming metallic nanoparticles.

The application of pure and modified TiO_2 NPs and colloids in surface modification of textiles has widely been investigated [19, 20]. For instance, the surface of wool fabrics was treated with commercial TiO_2 powder (P-25) and different characteristics such as photo-induced hydrophilicity [21], photo-yellowing [22], stain-removal [23], and anti-shrinkage [24] properties were explored. P-25 nanoparticles immobilised on the surface of fabrics using cross-linking agents such as 1,2,3,4, butane tetra carboxylic acid [23, 25], citric acid [22], maleic acid [26], succinic acid [27], and 1,2,3 propane tricarboxylic acid [27]. TiO_2 nanocoatings developed via the sol-gel method has also been reported, forming thin coating layers on fibres [28]. There are several reports on the synergistic impacts of Au dopants on photocatalytic activity of doped TiO_2 on textiles. Uddin

et al. [29] developed Au/TiO_2 coatings on cotton fabrics through a three-step treatment including synthesis of TiO_2 colloid, immersing the fabric into 0.001M $HAuCl_4$ solution, and 30 min irradiation (50 mW/cm^2, 295–3000 nm). A faster degradation of methylene blue (MB) dye was obtained under simulated sunlight; however, no actual test on the self-cleaning property of fabrics especially under visible light was conducted. Abdi et al [30] chemically reduced Au NPs on the surface of cotton fabric and then coated with a layer of anatase TiO_2. They reported enhanced photocatalytic discoloration of Remazol Blue dye solution in the presence of TiO_2/Au coated cotton fabric under a xenon light source. They reported that the order of surface treatment of fabric was effective on the overall photocatalytic activity where for the sample which was initially treated with TiO_2 and then post-treated with Au precursor, a weaker photocatalytic activity was observed [30]. Pakdel et al [31, 32] synthesised metal-doped TiO_2 and TiO_2/SiO_2 colloids without using any photoreduction and applied to the surface of wool and cotton fabrics. It was demonstrated that an optimum amount of metal dopants such as silver (Ag), platinum (Pt), and Au enhanced photocatalytic self-cleaning activity under both UV and visible light [32, 33]. The photoreduction method has been used for developing TiO_2 colloids modified with noble metals for textile applications. For example, Moridi-Mahdieh *et al.* [34] prepared Ag/TiO_2 (Ag/P-25) impregnating bath through a photoreduction method and used it for the treatment of polyester/cotton fabric via a dip-pad-dry-cure method. A significant improvement in the discoloration of treated fabrics was observed where the MB stain was removed from the fabric surface after 24 h exposure to sunlight. Montazer et al [35] synthesised Ag/TiO_2 nanocomposites via the photoreduction process and used it as an enhanced antimicrobial agent on wool fabric. The coated wool fabric showed superior antibacterial activity against *S. aureus* and *E. coli* bacteria.

Although there are numerous publications regarding the development of visible-light active nanocoatings on textiles, developing self-cleaning and antibacterial textiles using Au-doped TiO_2 colloids has rarely been reported. Further research is also required to elucidate the effect of the photoreduction process on the novel functionalities resulted from Au-doped TiO_2 coatings. Moreover, the synergistic effects of Au dopants with silica and its superhydrophilic effect on different characteristics of fabrics warrant further investigations. To address these drawbacks, this research investigates the effect of the synthesis approach of Au-doped TiO_2 colloids on the functionalities of cotton fabrics coated with TiO_2/Au and TiO_2/Au/SiO_2 colloids. Au was used as a dopant due to its high efficacy in improving the photocatalytic property of TiO_2, providing SPR effect, easy synthesis process, and biocompatibility, among others [17, 36]. The roles of several factors such as the photoreduction process, concentration of Au dopant, and the presence of silica on different properties of fabrics such as self-cleaning property under UV and visible light, antibacterial activity against *S. aureus* and *E. coli* bacteria, water absorption, and UV protection are discussed. Moreover, the surface characteristics of fabrics are studied using XPS, FTIR, SEM, and EDX techniques.

2. Experimental

2.1. Materials and chemicals

A 100% plain weave cotton fabric with the fabric mass of 135 g/m^2, and warp and weft linear densities of 34 and 37 tex, respectively, was used as substrate. The number of warp and weft yarns in the structure of fabric was 32 and 25 threads/cm, respectively. Titanium tetra isopropoxide (TTIP) 97% and tetra ethylorthosilicate (TEOS) 98% were used as the precursors of TiO_2 and SiO_2, respectively (Sigma-Aldrich). Gold (III) chloride trihydrate ($HAuCl_4 \cdot 3H_2O$) 99.9% was purchased from Sigma-Aldrich and was used as the precursor of Au NPs.

2.2. Synthesising TiO_2 and TiO_2/Au colloids

All colloids were synthesised through a low-temperature sol-gel method as reported earlier [33, 37]. 5% TiO_2 sol was synthesised through the reaction of TTIP (12.5 ml) with the mixture of acetic acid (12.5 ml) and water at 60°C. After mixing the solution, 1 ml nitric acid (HNO_3, 70%) was added to the solution and the transparent sol was stirred for 2 h at 60 °C. TiO_2/Au colloids were synthesised by adding a predetermined amount of metal precursor to the mixture. Two concentrations of gold precursor based on the molar ratios of Au:Ti: 0.001 and 0.01 were utilised in synthesising the sols. To be more concise, the terms of Au 0.001 and Au 0.01 will be used throughout this paper for the used concentrations of Au dopant. After adding HNO_3 into the mixture, the solution was stirred at 60°C for 2 h to obtain a transparent colloid. TiO_2/Au/SiO_2 colloids based on molar ratios of TTIP:TEOS 1:1 and 1:2.3 were prepared through adding SiO_2 sol to the TiO_2/Au colloid followed by 1 h mixing at room temperature. The SiO_2 sol was produced by adding TEOS in acidic water (pH=3) with a molar ratio of 1:20, followed by mixing for 2 h at room temperature. Two colloids were synthesised for each formulation, one of which was exposed to UVA for 1h to obtain the photoreduced colloid. The colloids which were prepared without photoreduction step and contained ionic gold were named as ionic-gold-doped (iGD) colloids, while the photoreduced ones were labelled as PR-colloids as listed in Table 1.

Table 1: The list of binary TiO_2/Au and ternary TiO_2/Au/SiO_2 colloids

	Ionic-gold-doped (iGD) colloids		**Photoreduced (PR)-method**
1	TiO_2/Au 0.001-iGD	**7**	TiO_2/Au 0.001-PR
2	TiO_2/Au 0.01-iGD	**8**	TiO_2/Au 0.01-PR
3	1/0.001/1-iGD	**9**	1/0.001/1-PR
4	1/0.01/1-iGD	**10**	1/0.01/1-PR
5	1/0.001/2.3-iGD	**11**	1/0.001/2.3-PR
6	1/0.01/2.3-iGD	**12**	1/0.01/2.3-PR

2.3. Surface coating of fabrics

The synthesised colloids were applied to cotton fabrics via a dip-pad-dry-cure process [38]. First, all cotton fabrics were scoured in the washing bath containing 2g/l detergent (Kieralon F-OL-B) in a liquid to fabric ratio of 50:1 at 40°C for 20 min in order to remove the surface impurities and wax. Dry samples were immersed into the prepared colloids and then padded with an automatic horizontal padding machine with a rotating speed of 7.5 rpm with the roller's nip pressure of 2.75 kg cm^{-2}. The coated fabrics were then neutralised with the fume of ammonia hydroxide 25% obtaining pH=7 on the fabrics. The drying process was carried out at 80°C for 5 min in an oven. The fabrics were cured at 120°C for 2 min to fix the applied nanoparticles on fabrics surface [39].

2.4. Self-cleaning test

Cotton samples were stained with 1 μL concentrated coffee and red-wine stains and exposed to UVA and visible light irradiation [33]. The UV-induced self-cleaning was tested under nine BLB bulbs of Philips TL-D 18 W with the maximum λ at 370 nm. The visible light was produced using a suntest solar simulator (Heraeus Suntest Solar CPS) fitted with a xenon arc source and equipped with a glass filter which cut out the UV part of the solar spectrum and generated light with a peak intensity at λ=470 nm [33]. The photographs of the fabrics were recorded after 3, 6, and 10 h of irradiation period.

2.5. Wet photocatalytic activity

1g of coated fabrics was cut into 1 cm ×1 cm pieces and added to a beaker containing 25 ml MB solutions (10 g/l, pH=1) [32]. Fabrics were mixed for 1 h in dark before irradiation to achieve adsorption-desorption equilibrium. The samples were irradiated under UVA and visible light sources while stirring. The UVA light was produced using the same set-up explained above and the visible light was generated by nine white, fluorescent lamps (Philips 30 W). The concentration of MB dye at different intervals was measured (C_t) using UV–vis

spectrophotometer (Varian-carry 300) and the dye concentration change compared with the initial dye concentration (C_0) was calculated based on Eq. 1. Moreover, the photocatalytic degradation kinetics were analysed based on pseudo-first (Eq 2) [31, 40] and pseudo-second order[41] (Eq 3) kinetic equations.

$$\text{Dye degradation (\%)} = [(C_0-C_t)/C_0]\times 100 \qquad \text{(Eq.1)}$$

$$-\ln (C_t/C_0)=k_1 t \qquad \text{(Eq 2)}$$

$$1/C_t= 1/C_0+k_2 t \qquad \text{(Eq 3)}$$

where k_1 and k_2 were reaction rate constants of dye degradation process based on pseudo-first and pseudo-second order kinetic models, respectively.

2.6. Antibacterial test

Antibacterial activity of fabrics was assessed against Gram-negative *Escherichia coli (E. coli*) and Gram-positive *Staphylococcus aureus (S. aureus)* bacteria based on AATCC 100-2004 test method [42]. Fabrics were cut circular with a diameter of 48 mm and sterilised under UV light for 45 min. The bacterial suspension with the concentration of 1×10^5 colony forming units (cfu)/ml was prepared by adding microorganisms into tryptic soy broth. Each fabric was put in a sterile gamma container and 1 ml of bacteria inoculum was added followed by incubation at 37 °C for 24 h. Next, 100 ml of normal saline was added to each container followed by vigorous shaking, and then 1 ml of the prepared solution was cultured in petri-dishes containing tryptic soy agar medium. The petri-dishes were incubated at 37 °C for 24 h and then the growth rate of bacteria colonies in each agar plate was observed and their photographs were recorded.

2.7. Washing fastness test

The washing fastness test was carried out using a laundry machine Ahiba IR Pro-dying machine (USA) based on the AATCC 61-2010 standard test method. Each piece of cotton fabric (10 cm×5 cm) was washed in separate canister of laundering machine in the presence of 200 ml

water containing 0.35% detergent and 10 steel balls at 40°C for 45 min. The washed samples were rinsed thoroughly with distilled water and dried in an oven at 50°C for 1h and kept in the laboratory for 12h before characterisation. The changes of UV-transmittance as well as UPF values of cotton fabrics were used to analyse the stability of nanoparticles applied to fabrics.

2.8. Characterisation techniques

The surface morphology and elemental analysis of fabrics were analysed using scanning electron microscopy (SEM) images and the energy dispersive X-ray (EDX) spectra using Zeiss Supra 55VP (Germany). High magnification images were taken using the same instrument using the In-Lense detector using 5 kV at the working distance of 3 mm. The surface of coated fabrics was characterised using X-Ray Photoelectron Spectroscopy (Thermo Fisher Scientific Nexsa) technique, and atomic ratios of detected elements on the outer surface of coatings were calculated. Fourier transform infrared spectroscopy (FTIR) analysis of samples was conducted using a Varian 1000 (Australia) instrument equipped with an attenuated total reflectance (ATR) accessory.

UV protection factor (UPF) of cotton fabrics was measured using a spectrophotometer (UPF and UV Penetration/Projection Measurement System, Model: YG902, China) according to the AS/NZS4399 standard [43]. The UPF values and UV transmittance rates in UVB and UVA regions were automatically calculated by the instrument. This test was conducted at least six times on different spots of each sample and the average values were reported.

The UV-vis reflectance spectra of fabrics were measured using a Carry 5000 UV-VIS-NIR spectrophotometer equipped with a diffuse reflectance accessory over 200-800 nm wavelength range.

WCA on fabrics was measured using KSV CAM101 instrument. The measured WCA was recorded at 0.2s after depositing the droplets on fabrics.

The band gap energy of all doped TiO_2 colloids was calculated using the Tauc relation based on the plot of $(\alpha h\upsilon)^{1/2}$ vs. $h\upsilon$ according to Eq 4 [44, 45].

$$(\alpha.h\nu)=A\,(h\nu-E_g)^{1/2} \qquad \text{(Eq. 4)}$$

where α was the energy-dependent absorption coefficient, hν was the incident photon energy, E_g was the band gap energy, and A was constant.

3. Results and discussion

3.1. Optical properties of colloids

UV-Vis absorption spectra shown in Figure 1 demonstrate the role of photoreduction process on the appearance of SPR peak of Au NPs. For TiO_2/Au-iGD colloids, which did not go through the photoreduction stage, no SPR peak was observed indicating the absence of metallic Au NP in the synthesised colloids [46, 47]. However, after 60 min of exposure to UVA, SPR peaks appeared at λ=545 and λ=570 nm for colloids containing Au 0.001 and 0.01, respectively. The addition of silica did not show a noticeable effect on the development of SPR peaks during the photoreduction stage and the peaks centered at the same maximum λ positions. However, the presence of silica in general enhanced the visible light absorption of colloids. This observation was consistent with the previous findings [38]. The concentration of $HAuCl_4$ was effective on the position of the SPR peak due to its influence on forming Au NPs with different particle sizes. For instance, the SPR peaks in PR-colloids which contained Au 0.001 as dopant appeared at shorter wavelengths, indicating the smaller particle sizes of the formed Au NPs. The photo-induced electrons from TiO_2 played a key role in reducing Au^{3+} ions into metallic Au NPs (Eq 5-9). Under UV irradiation, TiO_2 generated pairs of electrons and positive holes where the electrons moved to the surface of TiO_2 and either reacted with the surrounding $AuCl_4^-$ ions or recombined with positive holes. $AuCl_4^-$ ions then were transformed into Au^0 state and deposited as metallic Au NPs on the surface of TiO_2 after aggregation [46].

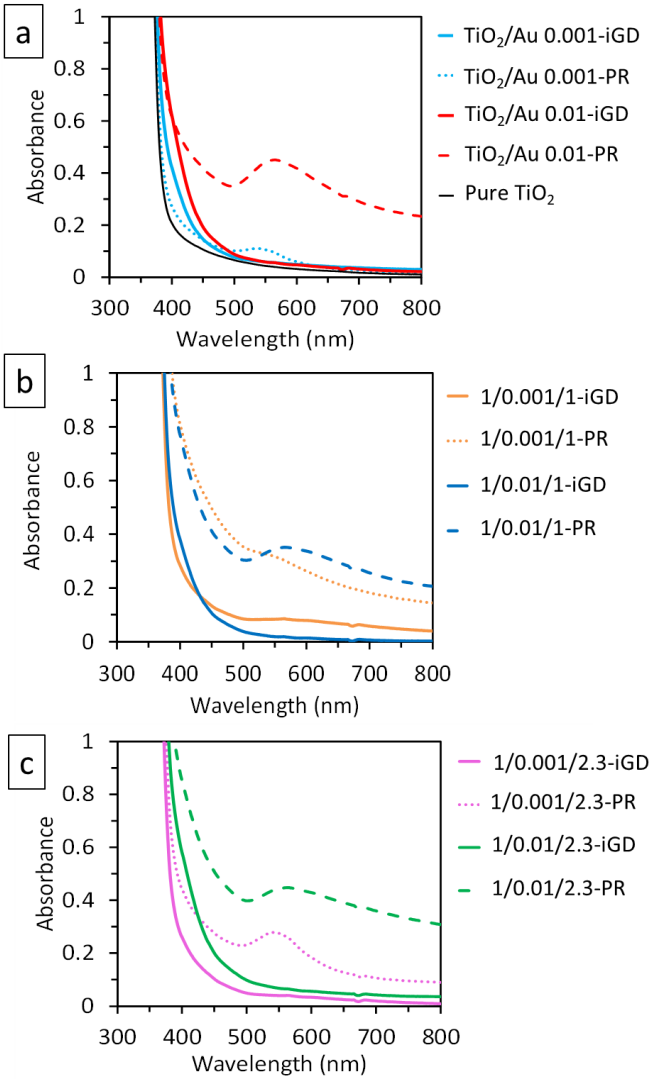

Figure 1: UV-Vis spectra of a) TiO_2/Au colloids, b and c) TiO_2/Au/SiO_2 colloids before and after photoreduction process

$TiO_2 + h\nu \rightarrow h^+ + e^-$ (Eq.5)

$AuCl_4^- + e^- \rightarrow AuCl_3^- + Cl^-$ (Eq.6)

$2AuCl_3^- \rightarrow AuCl_4^- + AuCl_2^-$ (Eq.7)

$AuCl_2^- + e^- \rightarrow Au^0 + 2Cl^-$ (Eq.8)

$nAu^0 \rightarrow (Au^0)_n$ (Eq.9)

The band gap energy of Au-doped samples was calculated (Figure S1). The band gap energy of a semiconductor such as TiO_2 indicates the energy required for triggering its photocatalytic activity [44]. Pure TiO_2 synthesised through the sol-gel method had a band gap energy of 3.10

eV. It was found that the concentration of $HAuC1_4$, and the synthesis method both determined the band gap energy of TiO_2/Au nanocomposites. Through doping TiO_2 with ionic Au 0.001, the band gap energy reduced to 3.05 eV indicating the introduction of Au impurity levels into the lattice of TiO_2 which led to modifying the band gap [48]. This can shift the activation threshold of TiO_2 NPs to longer wavelengths and visible region. However, the band gap of TiO_2/Au 0.01-PR was calculated to be around 3.11 eV which was even slightly larger than that of original TiO_2. The addition of silica to the system increased the band gap and did offset the effect of ionic Au 0.001 dopant in shortening the band gap (Table S1). The observed blue shift in the UV-vis spectra can be related to the effect of silica addition on reducing the aggregation of TiO_2 and TiO_2/Au NPs in the synthesised colloids. Our previous research showed that TiO_2/SiO_2 nanocomposites in general had a smaller crystallite size than pure TiO_2 [40]. This can result in a band gap increase based on the quantum size effect of semiconductors [40, 49]. Moreover, it has been reported that the existence of Ti–O–Si bonds in the structure of TiO_2/SiO_2 nanocomposites, can result in a blue shift in the calculated band gap energy [49]. This phenomenon can justify the observed larger band gap of $TiO_2/Au/SiO_2$ nanocomposites.

3.2. In-situ reduction of Au ions on fabrics

The synthesised colloids were applied to cotton fabrics via a dip-pad-dry-cure process and the effect of photoreduction process on characteristics of fabrics was investigated (Figure 2). One of the influenced aspects was the colour of the treated fabrics which changed depending on the concentration of ingredients in the colloids, and the synthesis method of colloids.

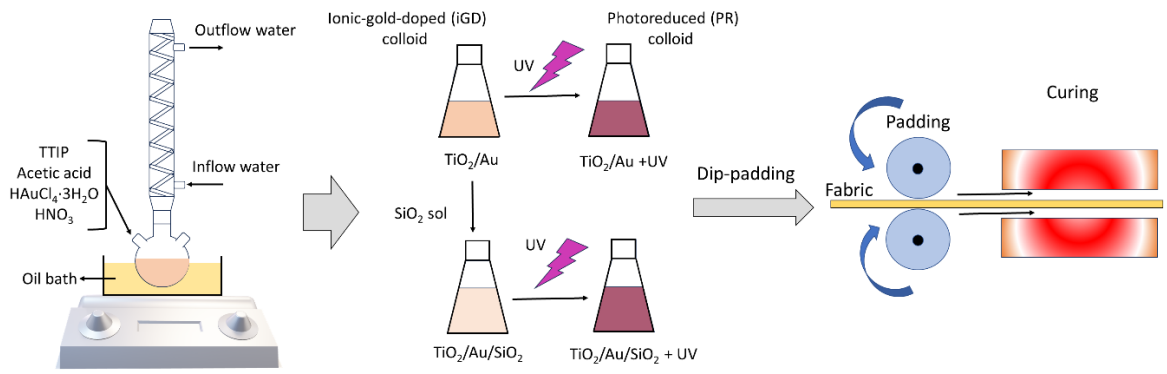

Figure 2: Schematic illustration of synthesis of Au-doped colloids and treatment of fabrics

A severe colour change was developed in cotton fabrics after treatment with colloids containing Au 0.01 as dopant. The colour change was stronger on fabrics treated with ionic colloids compared with the samples treated with photoreduced colloids (Figure 3a). This phenomenon can be related to the in-situ reduction of Au ions into Au NPs on the cellulosic substrate due to the existence of abundant hydroxyl groups on cotton structure which acted as reducing agents for Au salt [50-52]. Under this condition, Au^{3+} ions were transformed to metallic Au^{0} on the surface of cotton fibres [52]. The more noticeable colour changes of cotton fabrics treated with ionic colloids can be related to the formation of different shapes, sizes and quantity of nanoparticles on cotton fibres compared with the samples treated with the photoreduced sols. Also, it is plausible to say that ionic colloids contained higher concentrations of Au^{3+} ions compared with the photoreduced colloids, since during the UV irradiation period a portion of Au^{3+} ions already transformed to Au^{0}, resulting in a milder colour change on fabrics. The green method of in-situ reduction of Au ions into metallic Au NPs using cellulosic materials has already been reported and it is considered as a method which can obviate the need for using toxic reducing agents such as sodium borohydride ($NaBH_4$), sodium citrate ($Na_3C_6H_5O_7$), and hydroxyl amine hydrochloride ($HONH_2 \cdot HCl$) [51]. To better clarify the role of cellulosic substrate on inducing the in-situ reduction, the synthesised TiO_2/Au 0.01-iGD and TiO_2/Au/SiO_2 1/0.01/2.3-iGD colloids were applied to wool fabrics, and no colour change in fabrics was observed (Figure

S2). The presence of Au NPs on the surface of cotton changed the diffuse reflectance spectra of fabrics (Figure 3b and c). All coated fabrics, regardless of the concentration of Au and silica, showed a lower reflectance than pristine cotton over the UV region (λ<400 nm) which was due to the intrinsic UV absorption behaviour of TiO_2 NPs [53]. Fabrics coated with ionic colloids showed lower light reflectance over visible wavelength region compared with their photoreduced counterparts due to the existence of a higher amount of Au NPs on fibres. Moreover, it was noticed that the presence of silica increased the reflectance over the visible region which was consistent with the brighter colour of corresponding fabrics.

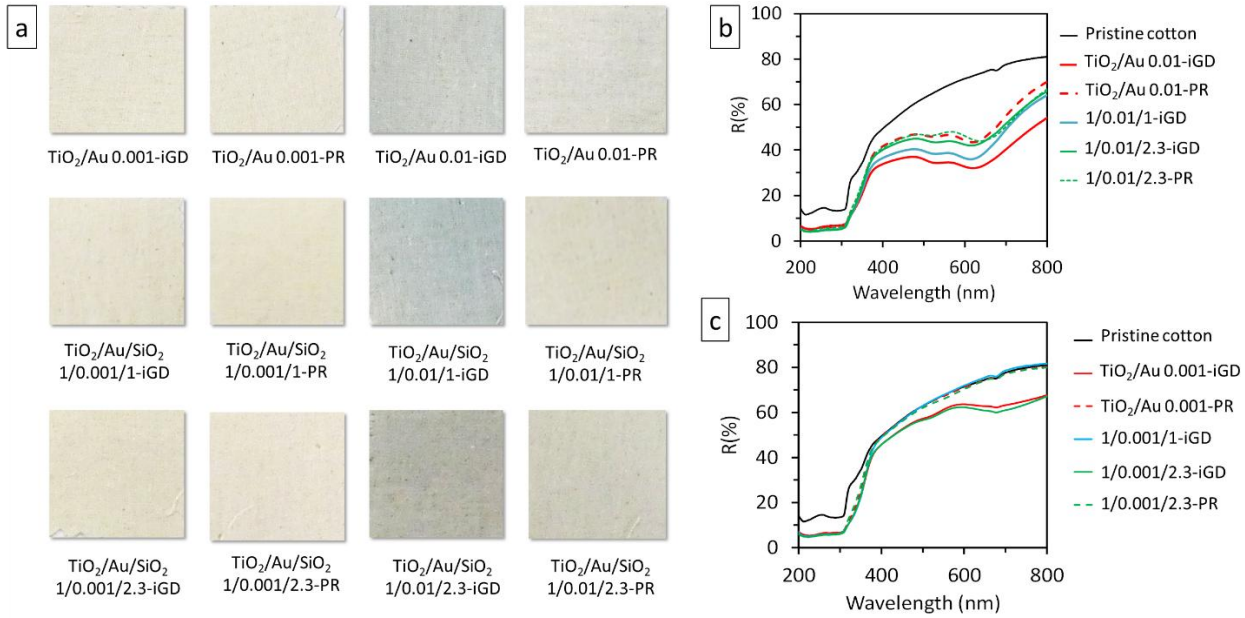

Figure 3: a) Photographs of cotton fabrics coated with Au-modified colloids, b) Diffuse reflectance spectra of cotton fabrics coated with colloids containing b) Au 0.01 and c) Au 0.001 as dopant.

3.3. Surface analysis

The elemental composition of applied coatings on the outer surface of fabrics was assessed (Figure 4). Four samples including pristine cotton, and coated with TiO_2/Au 0.01-PR, 1/0.01/1-iGD, and 1/0.01/2.3-iGD colloids were tested. In pristine cotton sample, only atoms of oxygen

(O1s) and carbon (C1 s) were detected. After applying binary and ternary colloids, the peaks related to Ti 2p and Si 2p appeared showing the successful coverage of fibres surface (Figure 4a-d). Based on the obtained high-resolution spectra of the fabric coated with TiO_2/Au (Figure 4e-i), the elements of Ti, O, C, and Au were detected. The peaks related to Ti $2p_{3/2}$ and Ti $2p_{1/2}$ appeared at 458.78 eV and 464.58 eV, respectively which are in good agreement with literature [54]. These peaks corresponded to Ti^{4+} bonds and proved the existence of TiO_2 on the surface [55]. The detected Au $4f_{7/2}$ peak at 83.3 eV confirmed the presence of metallic Au clusters on the coated surface; however, this peak could hardly be detected on the samples coated with colloids containing ionic gold [56]. The peak C1s in pristine cotton appeared as two main peaks at 284.78 eV and 286.28 eV which were related to C–C and C–H bonds, and C–O bond of cellulose, respectively [57]. After applying TiO_2-based colloids, the peak intensity at 284.78 eV increased which can be attributed to the formation of C–C bonds and the acetic acid [55]. Pristine cotton showed the O1s peak at 532.68 eV, while two peaks at 530.18 eV and 532.68 eV appeared for treated fabrics ascribing to TiO_2's lattice oxygen atoms, and surface hydroxyl group (Ti–OH), respectively [55, 58]. After adding SiO_2, the O1s peak intensity at 532.68 eV sharply increased, and the peak at 102.88 eV derived from Si–O–Si bond appeared [59]. The increase of peak intensity at 532.68 eV is ascribed to the formation of Si–O–Si and Ti–O–Si bonds, and hydroxyl groups from the surface [60]. The content of elements on some of the samples has been provided in Table S2.

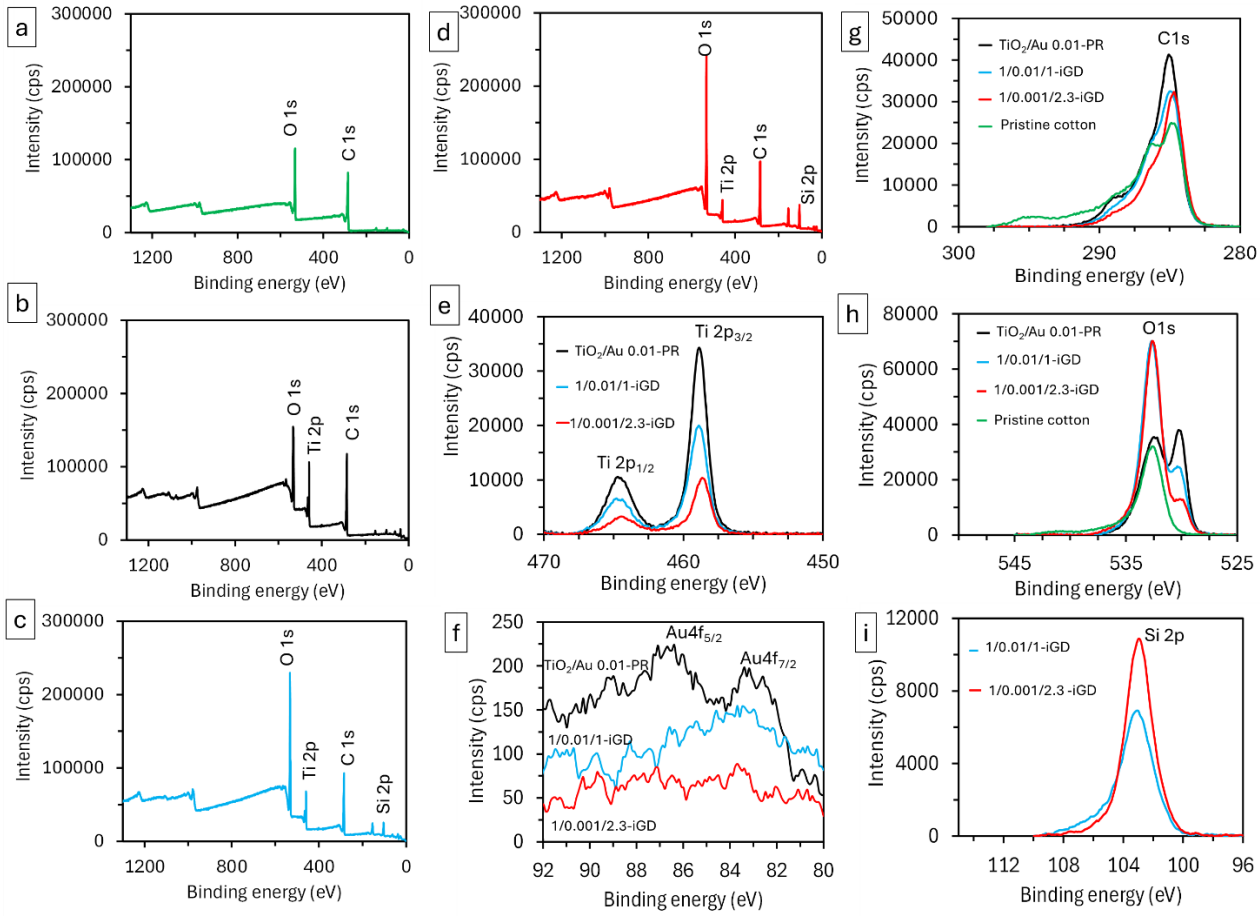

Figure 4: XPS survey spectra of a) pristine cotton; and cotton coated with b) TiO_2/Au 0.01-PR, c) 1/0.01/1-iGD, and d) 1/0.001/2.3-iGD colloids; high resolution spectra of e) Ti 2p, f) Au 4f, g) C 1s, h) O 1s, and i) Si 2p.

Figure 5a depicts the proposed mechanism for the attachment of applied coatings to the surface of cotton. Hydroxyl groups which are abundant in the structure of cellulose (Figure 5b) provide suitable binding sides for anchoring the applied TiO_2-based coatings to the surface [61]. Based on ATR-IR spectra shown in Figure 5c, pristine cotton showed the characteristic peaks at 3300 cm^{-1} and 2900 cm^{-1}, which were related to hydroxyl groups (OH) and C–O stretching vibrations of cellulose [62]. The peaks at 1715 cm^{-1}, 1100 cm^{-1} were related to the bending vibrations of carbonyl groups (C=O), and C–O bonds, respectively [62]. Applying the TiO_2-based colloids reduced the peak intensity at 3300 cm^{-1} which was related to bonding of cotton's surface hydroxyl groups with the applied coatings. The peaks related to the presence of SiO_2

and TiO_2 overlapped with characteristic peaks of pristine cotton in the range 800-1100 cm^{-1}. The peak intensity at around 1100 cm^{-1} increased after applying the TiO_2/Au/SiO_2 colloid, ascribing to the asymmetric stretching vibrations of the Si–O–Si, and implying the presence of silica on the surface of fabric. The small peak at 780 cm^{-1} was related to the symmetric stretching vibrations of Si–O–Si [40], and the shoulder peak appeared at 970 cm^{-1} was due to the presence of Ti–O–Si linkage[40].

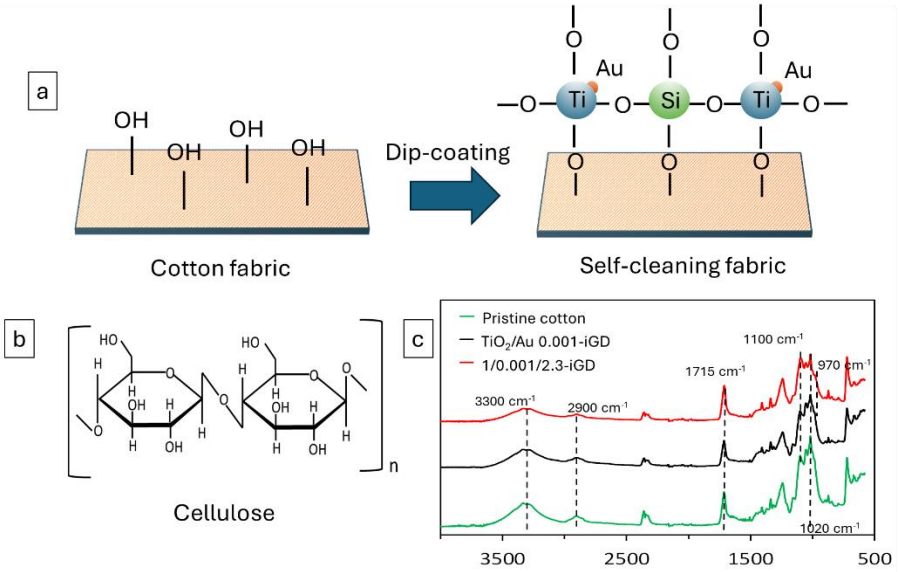

Figure 5: a) Proposed mechanism of the interaction of cotton fabric surface with the applied coatings, b) the structure of cellulose, c) FTIR spectra of coated fabrics

3.4. Effect of coatings on the wettability of fabrics

The application of coatings on cotton fabrics showed different impacts on wettability of fabrics depending on the ingredients of colloids (Figure 6). Pristine cotton fabric was hydrophilic, and the deposited water droplet formed the WCA 80.8° after contacting with the surface. This value increased after applying TiO_2/Au colloids implying that the fabrics became hydrophobic notwithstanding the synthesis procedure. However, after adding silica into colloids, the fabrics became superhydrophilic and the concentration of silica was important on the extent of superhydrophilicity. The fabrics coated with colloids containing Ti:Si 1:1 showed an initial

WCA around 20-30° after depositing the droplets on the surface. But by increasing the concentration of silica to Ti:Si 1:2.3 ratio, water droplets were instantly spread showing the superior superhydrophilicity.

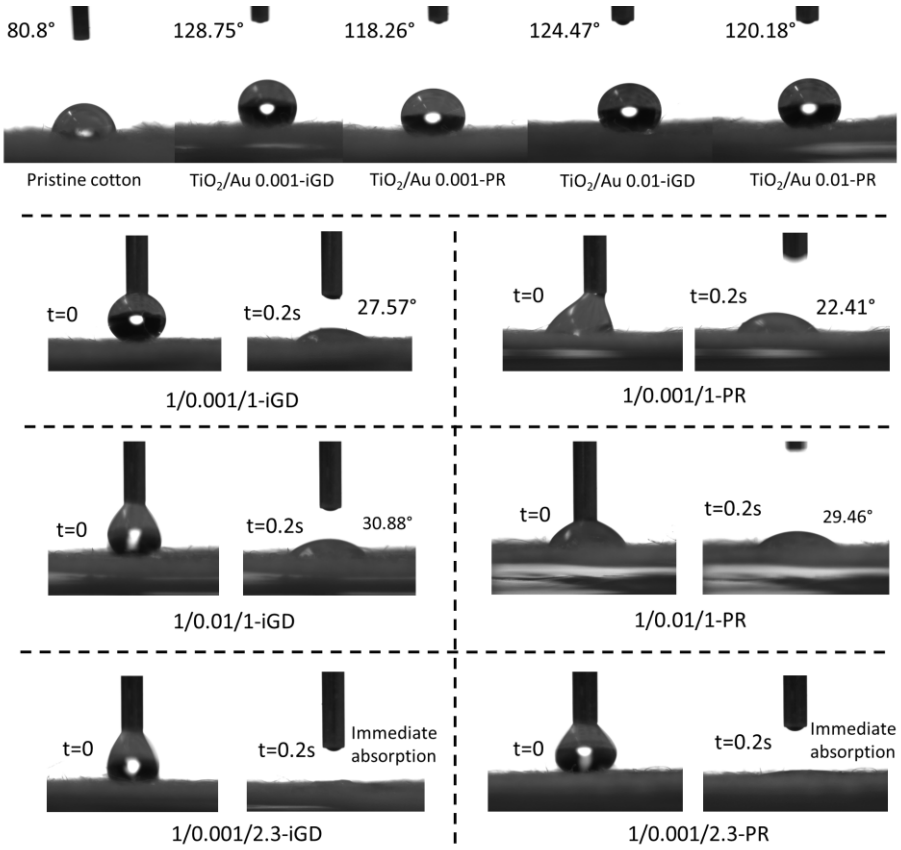

Figure 6: The variation of WCA on fabrics coated with TiO_2/Au and TiO_2/Au/SiO_2 colloids

3.5. Photocatalytic self-cleaning property of fabrics

The self-cleaning property of fabrics for the removal of coffee and red-wine stains was tested under two light sources of UVA and visible light, respectively. As a general trend, it was observed that the ionic Au-doped colloids showed a better photocatalytic activity in removal of stains (Figures 7 and 8). The presence of silica significantly boosted the photocatalytic self-cleaning effect due to its role in providing a better superhydrophilic effect on fabrics, increasing the surface area in the vicinity of TiO_2/Au photocatalysts, and increasing the surface acidity by creating Brønsted acid sites [38]. In addition, our previous research confirmed that TiO_2/SiO_2

colloids harnessed a greater amount of light than pure TiO_2 even in the visible region which can contribute to boosting the photocatalytic activity [7, 38]. In a superhydrophilic matrix, more water molecules are available in the surrounding environment of photocatalysts, and therefore the photogenerated electrons and holes can generate a greater population of reactive species of hydroxyl radials and superoxide anions. Moreover, increasing the concentration of silica from TiO_2/SiO_2 1:1 ratio to 1:2.3 was effective in enhancing the self-cleaning of TiO_2/Au colloids [38].

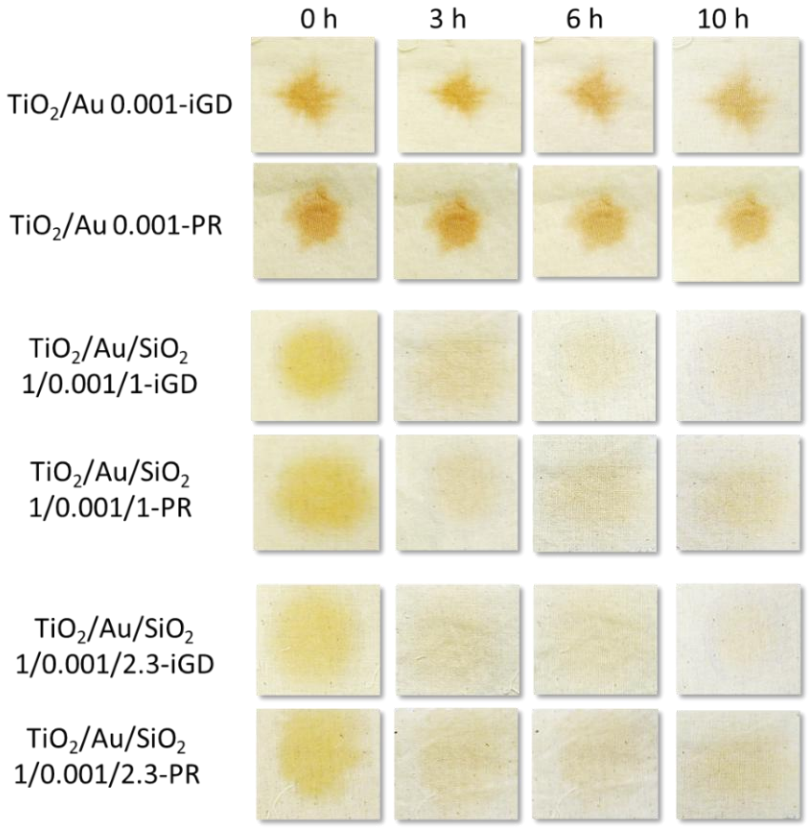

Figure 7: Photocatalytic coffee-stain removal on cotton fabrics under UV light

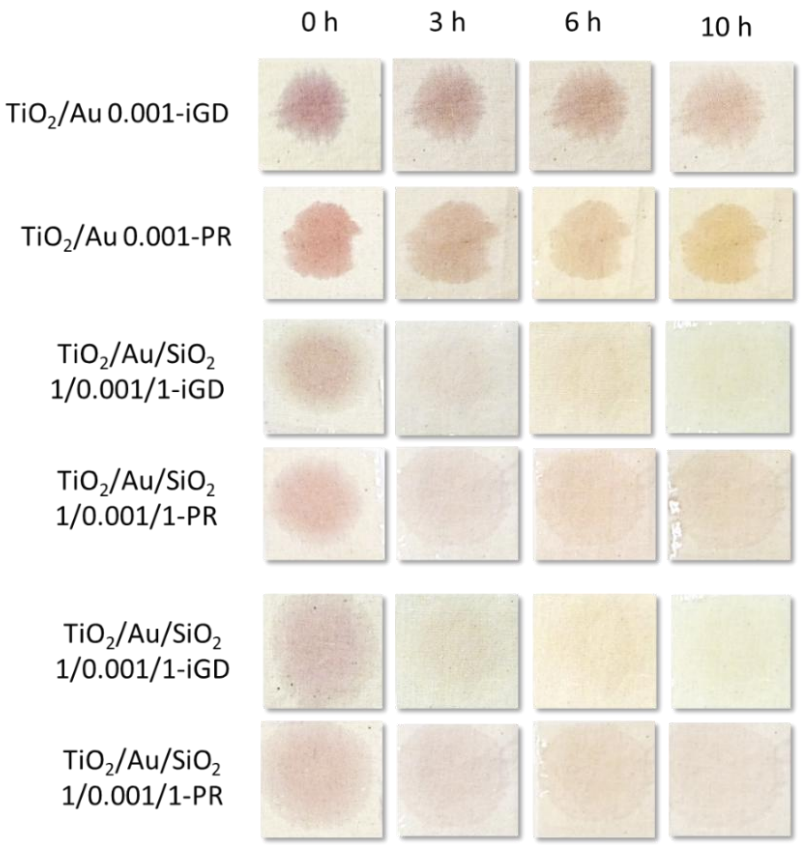

Figure 8: Photocatalytic red-wine-stain removal on cotton fabrics under visible light

The stain colour removal was obtained because of the photocatalytic activity of TiO_2 NPs (Eq 10-18). The self-cleaning performance was greatly affected by the presence of Au dopant and silica, although the effect of silica was more prominent. The Au dopants in the forms of ionic (Au^{3+}) and metallic (Au^0) acted differently in enhancing the photocatalytic activity of TiO_2 NPs (Figure 9). Under visible light irradiation, metallic Au contributed to the self-cleaning effect based on the SPR mechanism. Au NPs with SPR functionality can excite under visible light and inject electrons to the CB of TiO_2. The transferred electrons along with the created holes on Au NPs can react with surrounding environment producing reactive species to decompose contaminants [63]. However, under UV irradiation, the role of Au NPs in reducing the photogenerated electron-hole recombination is effective in enhancing the photocatalytic activity [64]. The deposited metallic Au NPs create Schottky barriers at the interface with TiO_2 easing the capture of generated electrons and therefore reducing the overall electron-hole

recombination [65]. This is due to the lower Fermi level of Au NPs, easing the transfer of photogenerated electrons from the CB of TiO_2 to the deposited Au NPs. This reduces the recombination of electron-hole pairs which enhances the photocatalytic activity [64]. The captured electrons can react with oxygen creating the reactive species to initiate the decomposition of organic pollutions [66]. These synergistic mechanisms boosted the self-cleaning functionality on the surface of coated fabrics. In addition, the ionic Au contributed to the photocatalytic self-cleaning by reducing the band gap energy of TiO_2, enhancing its responsiveness to longer wavelengths in the visible light region [67]. Also, Li and Li [68] demonstrated that the implantation of Au ions into the lattice of TiO_2 can result in reducing the electron-hole recombination due to the formation of new impurity energy level. Figure 9 illustrates the proposed mechanisms of the effects of ionic Au dopant and metallic Au NPs.

$TiO_2 + hv \rightarrow h_{VB}^+ + e_{CB}^-$ (Eq. 10)

$e_{CB}^- + h_{VB}^+ \rightarrow$ energy (Eq. 11)

$H_2O + h_{VB}+ \rightarrow \bullet OH + H^+$ (Eq. 12)

$O_2 + e_{CB}^- \rightarrow O_2\bullet^-$ (Eq. 13)

$\bullet OH$ + pollutant $\rightarrow\rightarrow\rightarrow H_2O + CO_2$ (Eq. 14)

$O_2\bullet^- + H^+ \rightarrow \bullet OOH$ (Eq. 15)

$\bullet OOH + \bullet OOH \rightarrow H_2O_2 + O_2$ (Eq. 16)

$O_2\bullet-$ + pollutant $\rightarrow\rightarrow\rightarrow CO_2 + H_2O$ (Eq. 17)

$\bullet OOH$ + pollutant $\rightarrow CO_2 + H_2O$ (Eq. 18)

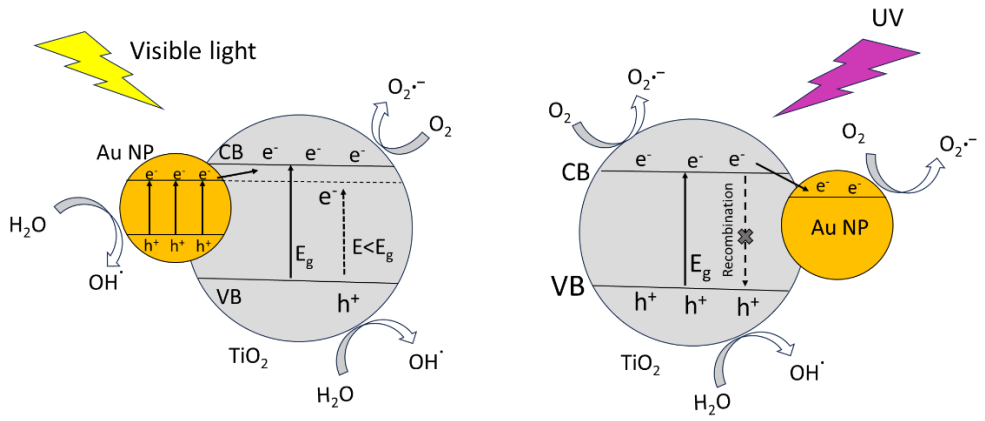

Figure 9: Photocatalytic mechanisms of Au-doped TiO_2 under visible light and UV

3.6. Wet photocatalytic activity and dye degradation kinetics

Photocatalytic activity of coated fabrics was quantitatively compared based on the degradation of MB dye under visible light (Figure 10). The samples were mixed with MB dye solution before starting the irradiation period. The concentration of control MB solution did not change during the irradiation period while in the presence of coated fabrics, its concentration dropped indicating the photocatalytic activity of fabrics. Among three tested set of samples, the binary TiO_2/Au treated fabrics showed the weakest photocatalytic dye degradation which was consistent with their self-cleaning performance. After introducing silica into the system, the dye absorption capacity of coated samples increased in relation to the silica content. The samples which were synthesised based on TiO_2/SiO_2 1:2.3 ratio showed the largest dye absorption during 1 h dark mixing step. Interestingly, the samples synthesised through the photoreduction method showed a lower initial dye uptake compared with the ionic colloid counterparts. Although their absorption difference was minor, this trend was observed for all tested fabrics regardless the content of silica. This can be related to the growth of Au NPs inside the porous structure of TiO_2/SiO_2 which limited the access of dye molecules to the pores and surface. The largest dye absorption during the dark mixing step was observed on the sample coated with TiO_2/Au/SiO_2 1/0.001/2.3-iGD colloid which reduced the dye concentration by 52.38%. The same sample showed the best photocatalytic dye degradation performance through reducing the dye concentration by 76.75%. In terms of photocatalytic activity, the samples treated with ionic TiO_2/Au colloids had a better photocatalytic activity under visible light compared with the samples treated with colloids synthesised via photoreduction. Using Au 0.01 as dopant instead of Au 0.001 was not beneficial in improving the photocatalytic activity notwithstanding the synthesis method.

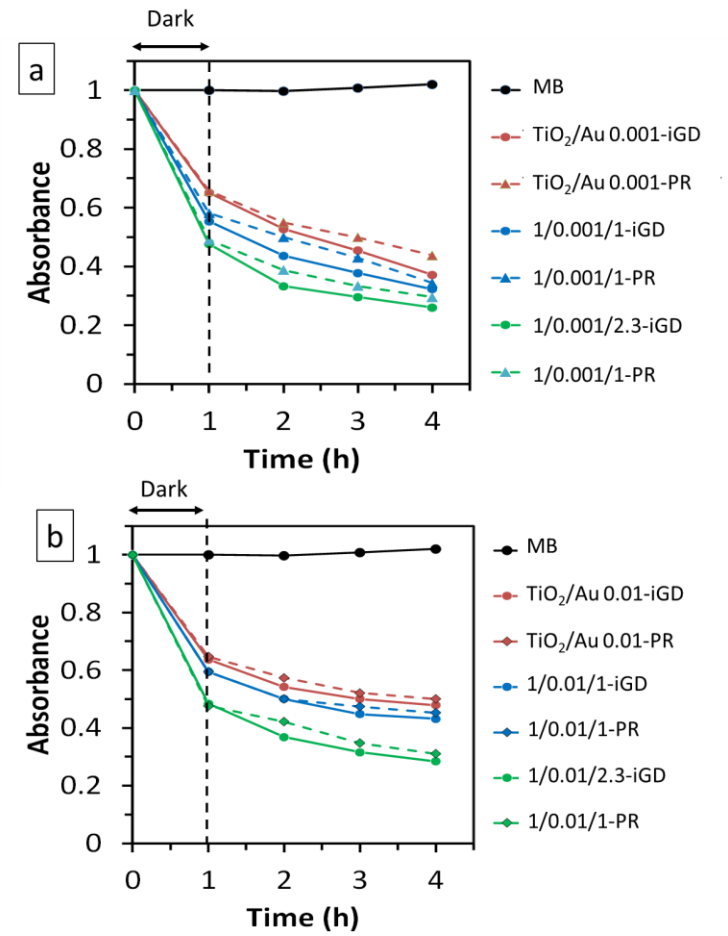

Figure 10: Photocatalytic MB dye degradation under visible light with fabrics treated with colloids containing a) Au 0.001 and b) Au 0.01 dopant

Analysis of dye degradation kinetics showed that the observed photocatalytic MB degradation was more inclined to be based on pseudo-second-order kinetic (Figure 11 and Table 2). All fabrics coated with ionic colloids led to a faster MB degradation compared with the samples treated with photoreduced colloids. This was confirmed based on the higher reaction rate constants of MB degradation in the presence of fabrics coated with ionic colloids. For instance, the reaction rate constant value (k_2) obtained for the fabric treated with TiO_2/Au 0.001-iGD was 0.0283 $L.g^{-1}.h^{-1}$, while this amount after photoreduction process decreased by 23.7% to 0.0216 $L.g^{-1}.h^{-1}$. Moreover, it was found that the dopant with the concentration of Au 0.001 was more effective than Au 0.01 in enhancing the photocatalytic activity under visible light. For instance, the sample coated with TiO_2/Au 0.001-iGD colloid showed 37.8% more efficient

photocatalytic activity than the sample treated with the colloid containing higher concentration of Au, i.e. TiO_2/Au 0.01-iGD. It has already been confirmed that in the presence of an excess amount of metal dopants, metals can reduce the photocatalytic activity of TiO_2 by acting as recombination centres for the generated electron-hole pairs [69].

Adding silica significantly contributed to increasing the photocatalytic MB dye removal. As a main effect, it significantly boosted the initial dye adsorption on fabrics. For instance, mixing dye with the fabrics treated with TiO_2/Au/SiO_2 1/0.001/1-iGD and 1/0.001/2.3-iGD colloids for 1 h in dark, resulted in 44.6 and 52.4% reduction in dye concentration, respectively. This is while only 34.9% dye removal was observed in the presence of fabric coated with TiO_2/Au 0.001-iGD after 1 h mixing in dark. For samples coated with ternary colloids containing silica, conducting the photoreduction process on colloids slowed the MB degradation and reduced the k_2 constant values. The MB degradation for the samples treated with 1/0.001/1-iGD and 1/0.001/1-PR were 68.8% and 55.3% colloids, respectively while their k_2 values were 0.0348 and 0.0471 based on the second-order kinetic model. Comparing the MB dye removal by ternary nanocomposites with binary TiO_2/Au colloids, it was observed that the overall k_2 values were much greater for the samples coated with silica-containing colloids. For instance, the fabrics coated with TiO_2/Au 0.001-iGD and TiO_2/Au/SiO_2 1/0.001/2.3-iGD colloids resulted in the k_2 constant values of 0.0283 and 0.0471 confirming the faster dye degradation in the presence of silica.

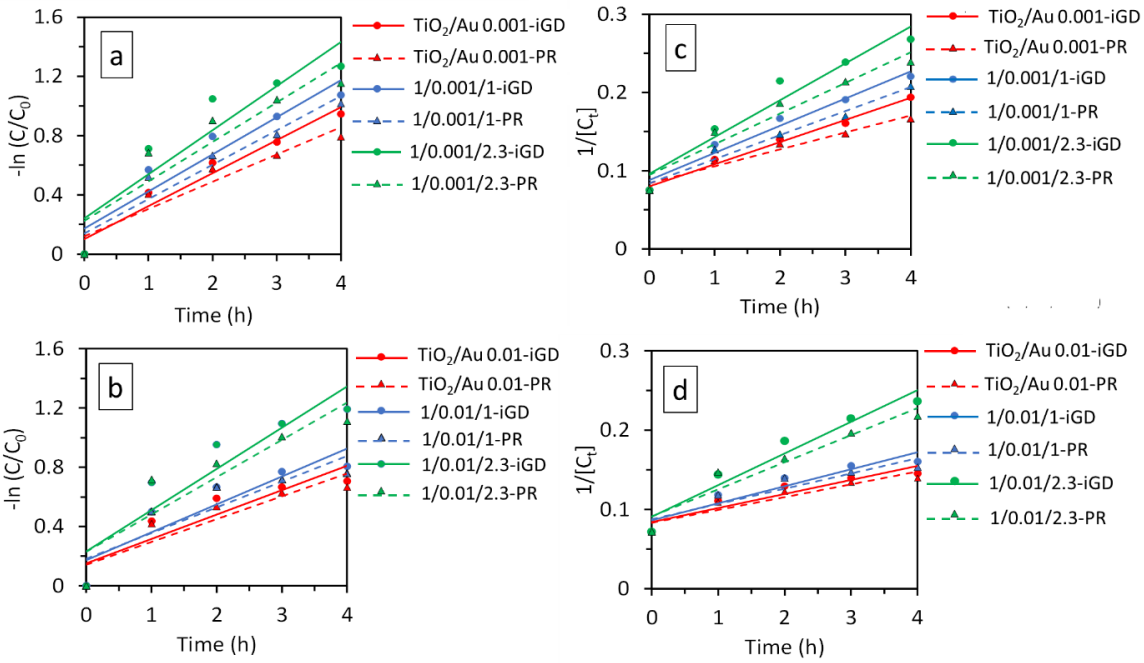

Figure 11: MB degradation kinetics under visible light; pseudo-first order kinetics with TiO_2/Au and TiO_2/Au/SiO_2 coated fabrics containing a) Au 0.001 and b) Au 0.01 dopant concentrations; and pseudo-second order kinetic with TiO_2/Au and TiO_2/Au/SiO_2 coated fabrics containing c) Au 0.001 and d) Au 0.01 dopant concentrations.

Table 2: MB dye degradation by TiO_2/Au and TiO_2/Au/SiO_2 colloids with and without photoreduction process based on pseudo-first and second-order kinetics

		First order kinetic		**Second order kinetic**	
Samples	MB concentration change (%)	k (h^{-1})	R^2	k (L. g^{-1}. H^{-1})	R^2
TiO_2/Au 0.001-iGD	61.13	0.2231	0.95	0.0283	0.99
TiO_2/Au 0.001-PR	54.67	0.1846	0.90	0.0216	0.96
1/0.001/1-iGD	65.81	0.2506	0.89	0.0348	0.97
1/0.001/1-PD	63.82	0.232	0.92	0.0308	0.97
1/0.001/2.3-iGD	71.89	0.298	0.85	0.0471	0.94
1/0.001/2.3-PD	68.5	0.267	0.85	0.0392	0.94
TiO_2/Au 0.01-iGD	50.71	0.1646	0.82	0.0176	0.88
TiO_2/Au 0.01-PD	48.66	0.1541	0.82	0.0161	0.88
1/0.01/1-iGD	55.31	0.1646	0.82	0.0214	0.89
1/0.01/1-PR	53.27	0.1738	0.78	0.0192	0.84
1/0.01/2.3-iGD	69.66	0.2785	0.85	0.04	0.94
1/0.01/2.3-PR	67.1	0.1882	0.82	0.0342	0.92

3.7. Antibacterial activity

Testing the antibacterial activity of cotton fabrics against both types of bacteria showed that the Au-modified coatings were not bactericidal. However, the colloids preparation method and the concentration of Au dopant were effective on the bacteria growth inhibition performance of coatings (Figure 12). As a general trend, it was observed that the photoreduction process reduced the antibacterial activity of coatings. This was consistent with results reported by Dasari *et al.* [70]. After applying TiO_2/Au 0.01 iGD colloid on cotton, a reduction in the growth of *E. coli* and *S. aureus* bacteria was observed, although the effectiveness against *S. aureus* seemed better. For this sample, the numbers of counted colonies of *E. coli* and *S. aureus* in petri dishes were 620 and 340 cfu/ml, respectively, while these numbers increased to 950 and 710 cfu/ml after undergoing a photoreduction step, for the fabric treated with TiO_2/Au 0.01-PR. Therefore, based on the number of colonies it can be said that the photoreduction process reduced the bacterial killing efficiency of fabrics by 53 % and 109% against *E. coli* and *S. aureus* bacteria, respectively. A similar trend was also observed on superhydrophilic fabrics where the 1/0.01/1-iGD sample showed superior antibacterial activity compared with the 1/0.01/1-PR fabric. There are various opinions about the mechanism of antibacterial activity of Au^{3+} ions and Au^0 NPs in the literature. It has been reported that metallic Au NPs usually have a high minimal inhibitory concentration to show antibacterial activity compared with other types of noble metals such as silver [71]. Weaker antibacterial activity of Au NPs results from the nature of gold which is biologically inert [72]. In general, several factors such as size, concentration, shape and surface characteristics of nanoparticle are determining factors on their antibacterial activity [71, 72]. As discussed, applying colloids containing ionic Au 0.01 led to the in-situ synthesis of Au NPs because of the reducing effect of cellulose. This process might have contributed to the better antibacterial effect. The presence of unreacted Au ions on the surface of fabrics which could interact with different components in cells walls and cause their

destruction might have contributed to the observed antibacterial effect. Moreover, different size and shape of the developed nanoparticles might have influenced on the obtained performance. On the samples coated with pure TiO_2 colloid and the colloids containing Au 0.001, no antibacterial activity was observed regardless of the synthesis method (Figure S3).

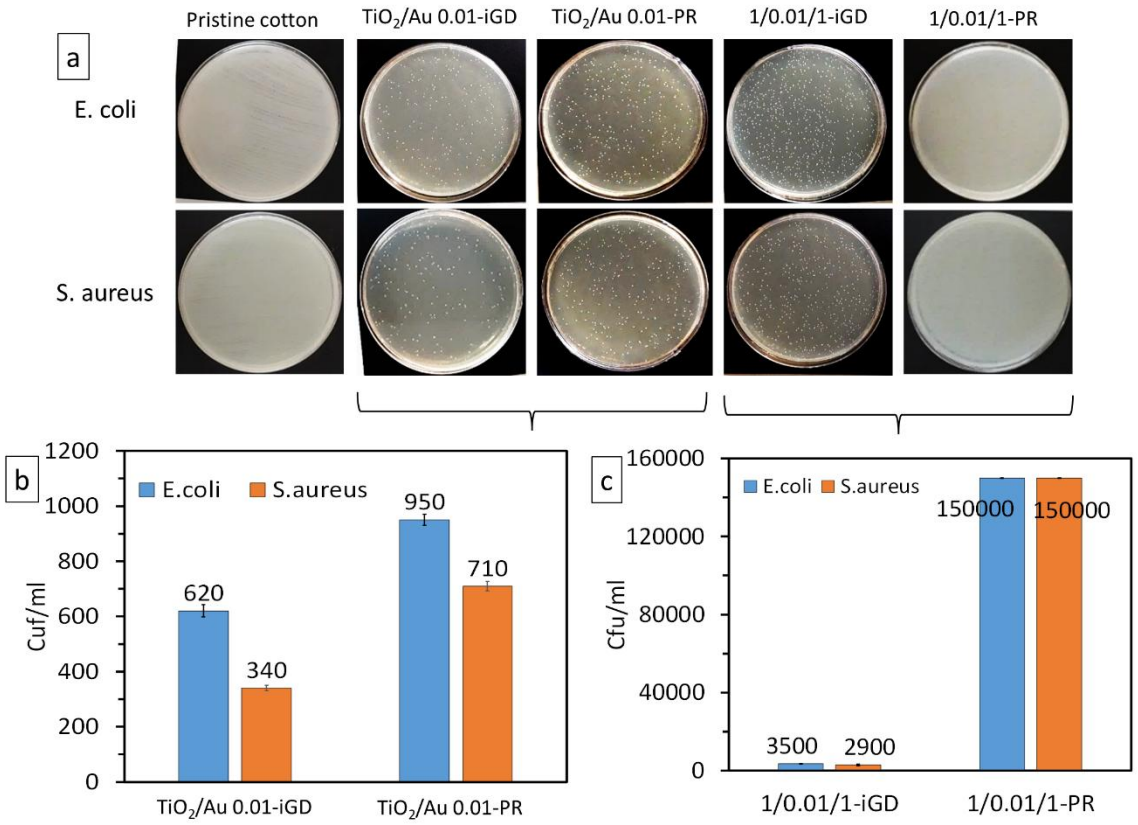

Figure 12: a) antibacterial activity of fabrics against *E. coli* and *S. aureus* bacteria, b and c) the number of formed bacteria colonies

3.8. UPF & washing fastness

The UPF of a textile determines the capability of the material in blocking UV radiation in the forms of absorption, reflection, and scattering [19]. The standard UPF rates are classified into three grades of good (15-24), very good (25-39), and excellent (40-50, and +50) [9, 73]. The applied Au-modified coatings boosted the UPF of cotton fabrics and as a general trend it was noticed that TiO_2/Au coatings showed higher UV blocking effectiveness compared with

TiO_2/Au/SiO_2 colloids (Figure 13). It was noticed that the fabrics coated with the photoreduced colloids had a modestly higher UPF levels compared with the samples treated with ionic colloids. The highest UPF level of 50.85 was achieved on the fabric coated with TiO_2/Au 0.001-PR colloid. Also, the effectiveness of the developed coatings in blocking UVA and UVB portion of solar spectrum was analysed (Figure S4). The results demonstrated that the binary TiO_2/Au colloids regardless of the synthesis method led to a reduced transmittance of both UVA and UVB radiations through the fabrics. Adding silica increased the transmission rates of both UVA and UVB through the fabrics, which explains the reason of the lower UPF of fabrics coated with ternary nanocomposites compared with the samples treated with TiO_2/Au colloids.

The enhanced UV protection property of fabrics can be explained based on the intrinsic UV absorption behaviour of TiO_2 NPs [74]. When TiO_2 absorbs incident UV light whose energy is greater than its band gap, it generates electron-hole pairs. These can be either involved in the photocatalytic reactions or be recombined releasing the absorbed energy. The former mechanism explains the reason of photocatalytic self-cleaning effect, and the latter mechanism is the reason of the improved UV protection level of TiO_2 coated fabrics [75]. By adding Au NPs with different particle sizes, different light scattering behaviour of applied coatings is expected which can explain the different UV protection level of fabrics [76].

To test the washing fastness of the most effective self-cleaning coating, i.e. the fabric coated with TiO_2/Au/SiO_2 1/0.001/2.3-iGD colloid, its UPF variation after five wash cycles was examined (Figures 13b and c). It was noticed that the UPF slightly increased during the 1st and 2nd wash cycles which can be related to the changes in the position of fibres and fabrics porosity after each wash cycle and the removal of physically attached nanoparticles. The UPF level was then remained stable during the next wash cycles. The UPF was 43.96 after 2nd wash while it changed to 38.82 after the 5th cycle. Obtaining high UPF levels after undergoing these intense wash cycles in the presence of detergent and steel balls confirmed the high durability of the

applied coatings even in the absence of any type of polymeric binder. Figure 13c shows that the UV-transmittance of the tested fabric did not have any major change during five wash cycles, confirming the existence of UV absorbing nanoparticles on the washed fabric.

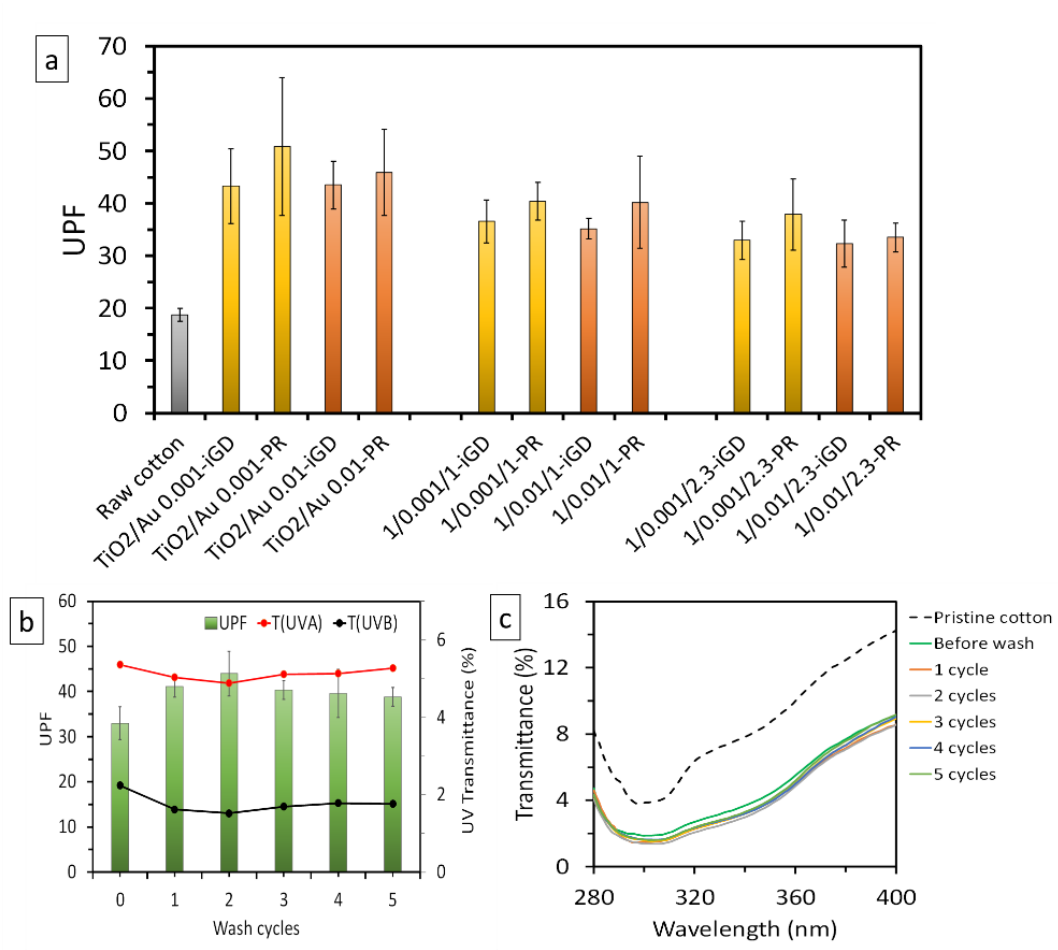

Figure 13: a) UPF levels of fabrics coated with TiO_2/Au and TiO_2/Au/SiO_2 colloids prepared based on Au 0.01 and Au 0.001 concentrations with and without photoreduction process, the variation of b) UPF level and c) UV transmittance of fabric coated with TiO_2/Au/SiO_2 1/0.001/2.3-iGD colloid

3.9. SEM images and EDX analysis

Based on SEM images (Figure 14), applying TiO_2/Au and TiO_2/Au/SiO_2 coatings led to the deposition of uniform and even coatings on cotton fibres. Changing the concentrations of Au dopant and silica, and the photoreduction process did not show tangible effects on the surface

morphology of coatings. No severe aggregation of nanoparticles was observed even after coating with high concentrations of silica. SEM images also confirmed the presence of TiO_2/Au/SiO_2 coatings on cotton fibres even after five wash cycles indicating the durability of coatings. No signs of destruction and non-uniformity were observed on the washed samples. To better understand the effect of colloids synthesis method on the surface morphology of coated fibres, images with higher magnification were prepared (Figure S5). It was noticed that the Au NPs existed on the surface of both groups of coated fibres, but their size was affected by the synthesis methods of colloids. Based on the particle size analysis, it was realised that the photoreduced TiO_2/Au 0.01-PR colloid led to the formation of Au NPs with the particle size around 130 nm. While the nanoparticles which were formed from the ionic colloid on fibres were in the size range of 15-25 nm. This may explain the different characteristics of fabrics such as colour shades, UV protection levels, and antibacterial activity. The different sizes of nanoparticles relate to their different formation mechanisms via photoreduction and in-situ reduction. The photoreduction process caused rapid growth and agglomeration of metal nanoparticles on the semiconductor surface, forming larger particle sizes. This can be explained through the tendency of nucleated metal nanoparticles in trapping the photo-generated charges under UV irradiation due to their lower Fermi level and the formed Schottky junctions at the interfaces [77]. Under this condition, the formed Au NPs act as preferential reduction sites for Au^{3+} ions [78]. Larger Au NPs scatter the incident UV light more effectively resulting in slightly enhnaced UV protection level [76, 79].

EDX spectra of the fabric coated with TiO_2/Au/SiO_2 1/0.001/2.3-iGD colloid confirmed the existence of Ti, Si, Au elements due to the presence of TiO_2, SiO_2, and Au NPs on the surface of fibres (Figure S6). The detection of elements on the washed sample corroborated the stability of applied coating.

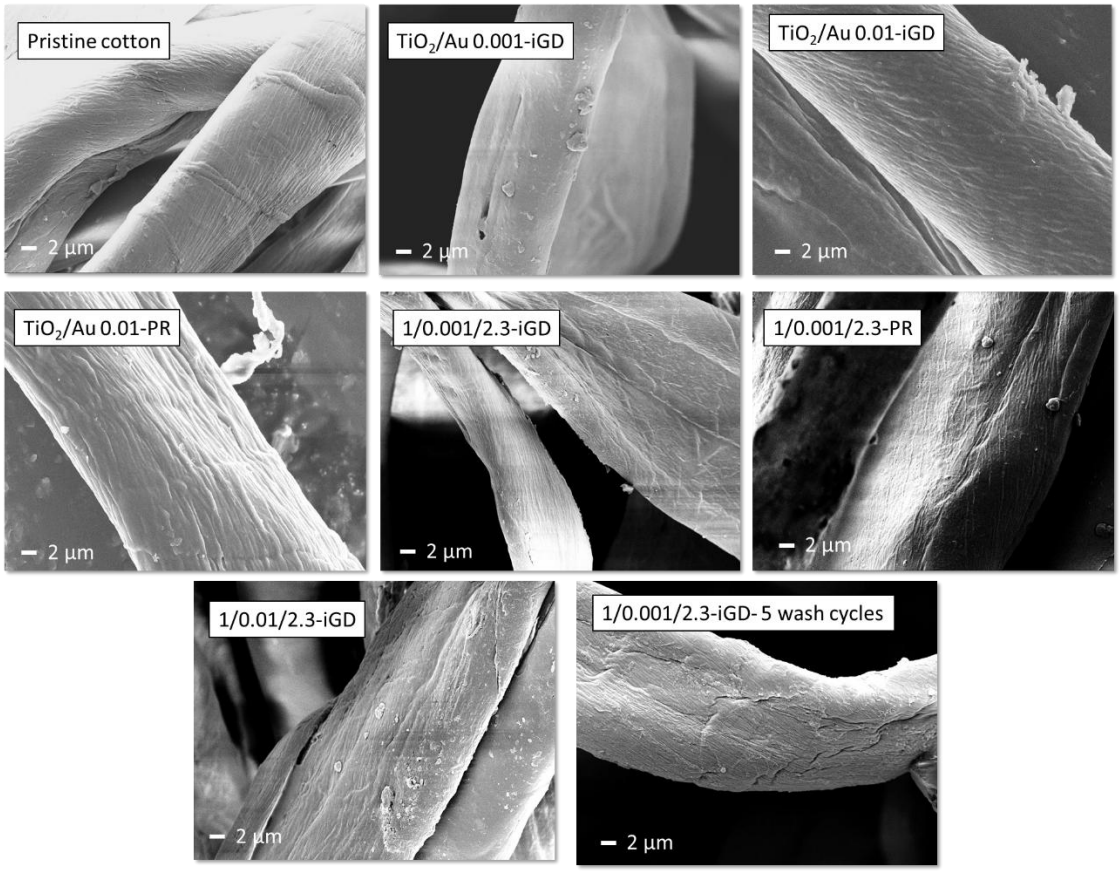

Figure 14: SEM images of pristine, coated and washed cotton fibres coated with TiO_2/Au and TiO_2/Au/SiO_2 colloids with ×2500 magnification.

Despite demonstrating high durability of the applied coatings on cotton, it is still required to get in-depth knowledge on biosafety aspects of these coated textiles. Previous research conducted by Tung et al [80] demonstrated the nonantiproliferative and noncytotoxic nature of textiles coated with pure TiO_2 colloids even up to 30% concentration on mouse embryonic fibroblasts. However, limited research has been conducted on the cytotoxicity of TiO_2/Au and TiO_2/Au/SiO_2 colloids and nanocoatings. Therefore, it is essential to examine the role of several factors such as the concentration of ingredients and composition of coating formulation, particles size, and synthesis method of gold-doped TiO_2 colloids on cells viability to further pave the way for practical applications of self-cleaning textiles in real-world applications.

4. Conclusion

In this study, TiO_2/Au and TiO_2/Au/SiO_2 colloids were synthesised through the sol-gel method and the effect of photoreduction process in developing self-cleaning, antibacterial activity and UV protection properties on cotton fabrics was examined. In addition, the effects of Au concentration and silica presence on photocatalytic MB dye degradation were investigated. The obtained results showed that the concentration of Au dopant and the synthesis approach both had key impacts on the functionalities of cotton fabrics. Compared with TiO_2/Au colloids, ternary TiO_2/Au/SiO_2 colloids produced more efficient photocatalytic capability for visible-light-induced self-cleaning functionality. It was found that the TiO_2/Au/SiO_2 coatings synthesised based on the molar ratios of Au:Ti 0.001 and Ti:Si 1:2.3 gave rise to a superior self-cleaning effect on cotton fabrics where coffee and red-wine stains were removed after 3 h of irradiation. Using ionic Au dopant with the molar concentration of Au:Ti 0.001 was the most effective in increasing the photocatalytic activity. But through further increasing the concentration to Au 0.01 and using the photoreduction process, the photoactivity of Au-doped coatings reduced. MB degradation on fabrics followed a pseudo-second order kinetic and the calculated reaction rate constants decreased after using the photoreduction step. Moreover, using an excess amount of Au dopant lowered the reaction rate constants and MB degradation amount. The synthesis approach was effective on the particle size of Au NPs where the particle size ranges of 130 nm and 15-25 nm were observed on samples coated with photoreduced and ionic colloids, respectively. Furthermore, it was revealed that the photoreduction of colloids had detrimental effects on the antibacterial activity of cotton fabrics against *E.coli* and *S. aureus* bacteria. TiO_2/Au/SiO_2 coating showed high durability on fabrics where the UV protection of fabrics did not deteriorate after five wash cycles.

Acknowledgement

This work was supported in part by the Research Centre of Textiles for Future Fashion at The Hong Kong Polytechnique University. We also wish to acknowledge research support from the Hong Kong Jockey Club Charities Trust.

Supporting Information

Band gap energy of TiO_2 and TiO_2/Au; Table of band gap energy levels for ternary nanocomposites; Photographs of wool fabrics coated with Au-doped colloid; Atomic ratios of elements on fabrics based on XPS test; Antibacterial test of samples coated with TiO_2 and colloids containing Au 0.001; UVA and UVB radiations transmitted through the fabrics; High magnification SEM images of coated fibres; EDX spectra of coated cotton fabrics.

Declaration of Competing Interest

None.

CRediT authorship contribution statement

E. Pakdel: Conceptualisation, Methodology, Investigation, Writing - original draft, Data curation. **W. A Daoud**: Supervision, methodology, Writing-review & editing. **X. Wang:** Supervision, Writing - review & editing.

References

(1) Pakdel, E.; Sharp, J.; Kashi, S.; Bai, W.; Gashti, M. P.; Wang, X. Antibacterial Superhydrophobic Cotton Fabric with Photothermal, Self-Cleaning, and Ultraviolet Protection Functionalities. *ACS Appl. Mater. Interfaces* **2023**, *15* (28), 34031-34043.
(2) Pakdel, E.; Fang, J.; Sun, L.; Wang, X. Nanocoatings for Smart Textiles. In Smart Textiles: Wearable Nanotechnology, Yilmaz, N. D. Ed.; Wiley,, 2018; pp 247-300.
(3) Peeters, H.; Keulemans, M.; Nuyts, G.; Vanmeert, F.; Li, C.; Minjauw, M.; Detavernier, C.; Bals, S.; Lenaerts, S.; Verbruggen, S. W. Plasmonic Gold-Embedded TiO_2 Thin Films as Photocatalytic Self-cleaning Coatings. *Appl. Catal. B* **2020**, *267*, 118654.
(4) Zhao, J.; Zhu, W.; Wang, X.; Liu, L.; Yu, J.; Ding, B. Environmentally Benign Modification of Breathable Nanofibrous Membranes Exhibiting Superior Waterproof and Photocatalytic Self-cleaning Properties. *Nanoscale Horiz.,* **2019**, *4* (4), 867-873.

(5) Yao, C.; Yuan, A.; Zhang, H.; Li, B.; Liu, J.; Xi, F.; Dong, X. Facile Surface Modification of Textiles with Photocatalytic Carbon Nitride Nanosheets and the Excellent Performance for Self-cleaning and Degradation of Gaseous Formaldehyde. *J. Colloid Interface Sci.* **2019**, *533*, 144-153.
(6) Zhang, J.; Li, L.; Li, H. Adsorption-Controlled Wettability and Self-Cleaning of TiO2. *Langmuir* **2023**, *39* (17), 6188-6200.
(7) Pakdel, E.; Daoud, W. A.; Wang, X. Self-cleaning and Superhydrophilic Wool by TiO_2/SiO_2 Nanocomposite. *Appl. Surf. Sci.* **2013**, *275*, 397-402.
(8) Banerjee, S.; Dionysiou, D. D.; Pillai, S. C. Self-cleaning Applications of TiO_2 by Photo-induced Hydrophilicity and Photocatalysis. *Appl. Catal. B: Environ.* **2015**, *176-177*, 396-428.
(9) Gashti, M. P.; Pakdel, E.; Alimohammadi, F. Nanotechnology-based Coating Techniques for Smart Textiles. In Active Coatings for Smart Textiles, Hu, J. Ed.; Woodhead Publishing, Duxford, 2016; pp 243-268.
(10) Wei, Y.; Wu, Q.; Meng, H.; Zhang, Y.; Cao, C. Recent Advances in Photocatalytic Self-cleaning Performances of TiO_2-based Building Materials. *RSC Adv.* **2023**, *13* (30), 20584-20597.
(11) Jeon, J.-P.; Kweon, D. H.; Jang, B. J.; Ju, M. J.; Baek, J.-B. Enhancing the Photocatalytic Activity of TiO_2 Catalysts. *Adv. Sustainable Syst.* **2020**, *4* (12), 2000197.
(12) Lu, X.; Li, Z.; Liu, Y. a.; Tang, B.; Zhu, Y.; Razal, J. M.; Pakdel, E.; Wang, J.; Wang, X. Titanium Dioxide Coated Carbon Foam as Microreactor for Improved Sunlight Driven Treatment of Cotton Dyeing Wastewater. *J. Clean. Prod.* **2020**, *246*, 118949.
(13) Basavarajappa, P. S.; Patil, S. B.; Ganganagappa, N.; Reddy, K. R.; Raghu, A. V.; Reddy, C. V. Recent Progress in Metal-doped TiO_2, Non-metal Doped/Codoped TiO_2 and TiO_2 Nanostructured Hybrids for Enhanced Photocatalysis. *Int. J. Hydrog. Energy* **2020**, *45* (13), 7764-7778.
(14) Zhao, J.; Wang, J.; Fan, L.; Pakdel, E.; Huang, S.; Wang, X. Immobilization of Titanium Dioxide on PAN Fiber as a Recyclable Photocatalyst via Co-dispersion Solvent Dip Coating. *Tex. Res. J.* **2017**, *87* (5), 570-581.
(15) Xie, W.; Pakdel, E.; Liang, Y.; Liu, D.; Sun, L.; Wang, X. Natural Melanin/TiO_2 Hybrids for Simultaneous Removal of Dyes and Heavy Metal Ions Under Visible Light. *J. Photochem. Photobiol., A* **2020**, *389*, 112292.
(16) Vanlalhmingmawia, C.; Lee, S. M.; Tiwari, D. Plasmonic Noble Metal Doped Titanium Dioxide Nanocomposites: Newer and Exciting Materials in the Remediation of Water Contaminated with Micropollutants. *J. Water Proc.engineering* **2023**, *51*, 103360.
(17) Etacheri, V.; Di Valentin, C.; Schneider, J.; Bahnemann, D.; Pillai, S. C. Visible-Light Activation of TiO_2 Photocatalysts: Advances in Theory and Experiments. *J. Photochem. Photobiol. C: Photochem. Rev.* **2015**, *25*, 1-29.
(18) Wu, H.; Liu, Y.; Chen, G.; Li, T.; Jiang, W.; Jia, R.; Zhang, M.; Yuan, S.; Shi, L.; Huang, L. Surface-Confined Photodeposition of Noble Metal Nanoclusters on TiO_2 in a Fluidized Bed for the Catalytic Oxidation of Formaldehyde. *ACS Appl. Nano Mater.* **2022**, *5* (9), 13100-13111.
(19) Rashid, M. M.; Simončič, B.; Tomšič, B. Recent Advances in TiO_2-Functionalized Textile Surfaces. *Surf. Interfaces* **2021**, *22*, 100890.
(20) Montazer, M.; Pakdel, E. Functionality of Nano Titanium Dioxide on Textiles with Future Aspects: Focus on Wool. *J. Photochem. Photobiol., C* **2011**, *12* (4), 293-303.
(21) Montazer, M.; Pakdel, E.; Moghadam, M. B. The Role of Nano Colloid of TiO_2 and Butane Tetra Carboxylic Acid on the Alkali Solubility and Hydrophilicity of Proteinous Fibers. *Colloids Surf., A* **2011**, *375* (1-3), 1-11.
(22) Montazer, M.; Pakdel, E. Reducing photoyellowing of wool using nano TiO_2. *Photochem. Photobiol.* **2010**, *86* (2), 255-260.
(23) Montazer, M.; Pakdel, E. Self-cleaning and Color Reduction in Wool Fabric by Nano Titanium Dioxide. *J. Text. Inst.* **2011**, *102* (4), 343-352.
(24) Montazer, M.; Pakdel, E.; Behzadnia, A. Novel Feature of Nano-Titanium Dioxide on Textiles: Antifelting and Antibacterial Wool. *J. Appl. Polym. Sci.* **2011**, *121* (6), 3407-3413.

(25) Montazer, M.; Pakdel, E.; Moghadam, M. Nano Titanium Dioxide on Wool Keratin as UV Absorber Stabilized by Butane Tetra Carboxylic Acid (BTCA): A Statistical Prospect. *Fibers Polym.* **2010**, *11* (7), 967-975.
(26) Lessan, F.; Montazer, M.; Moghadam, M. B. A Novel Durable Flame-Retardant Cotton Fabric Using Sodium Hypophosphite, Nano TiO_2 and Maleic Acid. *Thermochim. Acta* **2011**, *520* (1), 48-54.
(27) Meilert, K. T.; Laub, D.; Kiwi, J. Photocatalytic Self-cleaning of Modified Cotton Textiles by TiO_2 Clusters Attached by Chemical Spacers. *J. Mol. Catal. A: Chem.* **2005**, *237* (1-2), 101-108.
(28) Daoud, W. A.; Xin, J. H. Low Temperature Sol-Gel Processed Photocatalytic Titania Coating. *J. Sol-Gel Sci. Technol.* **2004**, *29* (1), 25-29.
(29) Uddin, M. J.; Cesano, F.; Scarano, D.; Bonino, F.; Agostini, G.; Spoto, G.; Bordiga, S.; Zecchina, A. Cotton Textile Fibres Coated by Au/TiO_2 Films: Synthesis, Characterization and Self cleaning Properties. *J. Photochem. Photobiol., A* **2008**, *199* (1), 64-72.
(30) Abid, M.; Bouattour, S.; Ferraria, A. M.; Conceição, D. S.; Carapeto, A. P.; Vieira Ferreira, L. F.; Botelho do Rego, A. M.; Rei Vilar, M.; Boufi, S. Functionalization of Cotton Fabrics with Plasmonic Photo-active Nanostructured Au-TiO_2 Layer. *Carbohydr. Polym.* **2017**, *176*, 336-344.
(31) Pakdel, E.; Daoud, W. A.; Sun, L.; Wang, X. Visible and UV Functionality of TiO_2 Ternary Nanocomposites on Cotton. *Appl. Surf. Sci.* **2014**, *321*, 447–456.
(32) Pakdel, E.; Daoud, W. A.; Afrin, T.; Sun, L.; Wang, X. Self-Cleaning Wool: Effect of Noble Metals and Silica on Visible-Light-Induced Functionalities of Nano TiO_2 Colloid. *J. Text. Inst.* **2015**, *106* (12), 1348-1361.
(33) Pakdel, E.; Daoud, W. A.; Varley, R. J.; Wang, X. Antibacterial Textile and The Effect of Incident Light Wavelength on Its Photocatalytic Self-Cleaning Activity. *Mater. Lett.* **2022**, *318*, 132223.
(34) Moridi Mahdieh, Z.; Shekarriz, S.; Afshar Taromi, F.; Montazer, M. A New Method for In situ Synthesis of Ag–TiO_2 Nanocomposite Particles on Polyester/Cellulose Fabric by Photoreduction and Self-cleaning Properties. *Cellulose* **2018**, *25* (4), 2355-2366.
(35) Montazer, M.; Behzadnia, A.; Pakdel, E.; Rahimi, M. K.; Moghadam, M. B. Photo Induced Silver on Nano Titanium Dioxide as an Enhanced Antimicrobial Agent for Wool. *J. Photochem. Photobiol., B* **2011**, *103* (3), 207-214.
(36) Elahi, N.; Kamali, M.; Baghersad, M. H. Recent Biomedical Applications of Gold Nanoparticles: A Review. *Talanta* **2018**, *184*, 537-556.
(37) Pakdel, E.; Daoud, W. A.; Afrin, T.; Sun, L.; Wang, X. Enhanced Antimicrobial Coating on Cotton and Its Impact on UV Protection and Physical Characteristics. *Cellulose* **2017**, *24* (9), 4003-4015.
(38) Pakdel, E.; Daoud, W. Self-cleaning Cotton Functionalized with TiO_2/SiO_2: Focus on the Role of Silica. *J. Colloid Interface Sci.* **2013**, *401*, 1-7.
(39) Afzal, S.; Daoud, W. A.; Langford, S. J. Photostable Self-cleaning Cotton by a Copper (II) Porphyrin/TiO_2 Visible-Light Photocatalytic System. *ACS Appl. Mater. Interfaces* **2013**, *5* (11), 4753–4759.
(40) Pakdel, E.; Daoud, W. A.; Seyedin, S.; Wang, J.; Razal, J. M.; Sun, L.; Wang, X. Tunable Photocatalytic Selectivity of TiO_2/SiO_2 Nanocomposites: Effect of Silica and Isolation Approach. *Colloids Surf., A* **2018**, *552*, 130-141.
(41) Qing, W.; Chen, K.; Wang, Y.; Liu, X.; Lu, M. Green Synthesis of Silver Nanoparticles by Waste Tea Extract and Degradation of Organic Dye in the Absence and Presence of H_2O_2. *Appl. Surf. Sci.* **2017**, *423*, 1019-1024.
(42) Pakdel, E.; Kashi, S.; Sharp, J.; Wang, X. Superhydrophobic, Antibacterial, and EMI Shielding Properties of Ag/PDMS-Coated Cotton Fabrics. *Cellulose* **2024**, *in press*.
(43) Pakdel, E.; Xie, W.; Wang, J.; Kashi, S.; Sharp, J.; Zhang, Q.; Varley, R. J.; Sun, L.; Wang, X. Superhydrophobic Natural Melanin-Coated Cotton with Excellent UV Protection and Personal Thermal Management Functionality. *Chem. Eng. J.* **2022**, *433*, 133688.
(44) Makuła, P.; Pacia, M.; Macyk, W. How To Correctly Determine the Band Gap Energy of Modified Semiconductor Photocatalysts Based on UV–Vis Spectra. *J. Phys. Chem. Lett.* **2018**, *9* (23), 6814-6817.

(45) Xu, J.; Li, L.; Yan, Y.; Wang, H.; Wang, X.; Fu, X.; Li, G. Synthesis and Photoluminescence of Well-dispersible Anatase TiO_2 Nanoparticles. *J. Colloid Interface Sci.* **2008**, *318* (1), 29-34.
(46) Wang, C.-y.; Liu, C.-y.; Zheng, X.; Chen, J.; Shen, T. The Surface Chemistry of Hybrid Nanometer-Sized Particles I. Photochemical Deposition of Gold on Ultrafine TiO_2 Particles. *Colloids Surf A.* **1998**, *131* (1), 271-280.
(47) Tahir, M.; Tahir, B.; Amin, N. A. S. Gold-Nanoparticle-Modified TiO_2 Nanowires for Plasmon-Enhanced Photocatalytic CO_2 Reduction with H_2 Under Visible Light Irradiation. *Appl. Surf. Sci.* **2015**, *356*, 1289-1299.
(48) Tahir, B.; Tahir, M.; Amin, N. A. S. Photocatalytic CO_2 Conversion over Au/TiO_2 Nanostructures for Dynamic Production of Clean Fuels in a Monolith Photoreactor. *Clean Techn Environ Policy* **2016**, *18* (7), 2147-2160.
(49) Ohno, T.; Tagawa, S.; Itoh, H.; Suzuki, H.; Matsuda, T. Size Effect of TiO_2–SiO_2 Nano-hybrid Particle. *Mater. Chem. Phys.* **2009**, *113* (1), 119-123.
(50) Li, Z.; Friedrich, A.; Taubert, A. Gold Microcrystal Synthesis via Reduction of $HAuCl_4$ by Cellulose in the Ionic Liquid 1-Butyl-3-Methyl Imidazolium Chloride. *J. Mater. Chem.* **2008**, *18* (9), 1008-1014.
(51) Tan, J.; Liu, R.; Wang, W.; Liu, W.; Tian, Y.; Wu, M.; Huang, Y. Controllable Aggregation and Reversible pH Sensitivity of AuNPs Regulated by Carboxymethyl Cellulose. *Langmuir* **2010**, *26* (3), 2093-2098.
(52) Haslinger, S.; Ye, Y.; Rissanen, M.; Hummel, M.; Sixta, H. Cellulose Fibers for High-Performance Textiles Functionalized with Incorporated Gold and Silver Nanoparticles. *ACS Sustainable Chem. Eng.* **2020**, *8* (1), 649-658.
(53) Pakdel, E.; Daoud, W. A.; Sun, L.; Wang, X. Photostability of Wool Fabrics Coated with Pure and Modified TiO_2 Colloids. *J. Colloid Interface Sci.* **2015**, *440* (0), 299-309.
(54) Topalovic, T.; Nierstrasz, V. A.; Bautista, L.; Jocic, D.; Navarro, A.; Warmoeskerken, M. M. C. G. XPS and Contact Angle Study of Cotton Surface Oxidation by Catalytic Bleaching. *Colloids Surf. A: Physicochem. Eng. Asp.* **2007**, *296* (1), 76-85.
(55) Milićević, N.; Novaković, M.; Potočnik, J.; Milović, M.; Rakočević, L.; Abazović, N.; Pjević, D. Influencing Surface Phenomena by Au Diffusion in Buffered TiO_2-Au Thin Films: Effects of Deposition and Annealing Processing. *Surf. Interfaces.* **2022**, *30*, 101811.
(56) Cojocaru, B.; Neaţu, Ş.; Sacaliuc-Pârvulescu, E.; Lévy, F.; Pârvulescu, V. I.; Garcia, H. Influence of Gold Particle Size on the Photocatalytic Activity for Acetone Oxidation of Au/TiO_2 Catalysts Prepared by dc-Magnetron Sputtering. *Appl. Catal. B: Environ.* **2011**, *107* (1), 140-149.
(57) Inbakumar, S.; Morent, R.; De Geyter, N.; Desmet, T.; Anukaliani, A.; Dubruel, P.; Leys, C. Chemical and Physical Analysis of Cotton Fabrics Plasma-treated with a Low Pressure DC Glow Discharge. *Cellulose* **2010**, *17* (2), 417-426.
(58) Bai, W.; Pakdel, E.; Wang, Q.; Tang, B.; Wang, J.; Chen, Z.; Zhang, Y.; Hurren, C.; Wang, X. Synergetic Adsorption-Photocatalysis Process of Titania-Silica Photocatalysts and their Immobilization on PEEK Nonwoven Filter for VOC Removal. *J. Environ. Chem. Eng.* **2022**, *10* (6), 108920.
(59) Hu, M.; Xing, Z.; Cao, Y.; Li, Z.; Yan, X.; Xiu, Z.; Zhao, T.; Yang, S.; Zhou, W. Ti^{3+} Self-doped Mesoporous Black TiO_2/SiO_2/g-C_3N_4 Sheets Heterojunctions as Remarkable Visible-Lightdriven Photocatalysts. *Appl. Catal. B: Environ.* **2018**, *226*, 499-508.
(60) Ren, C.; Qiu, W.; Chen, Y. Physicochemical Properties and Photocatalytic Activity of the TiO_2/SiO_2 Prepared by Precipitation Method. *Sep. Purif. Technol.* **2013**, *107*, 264-272.
(61) Zhang, J.; Li, L.; Li, Y.; Yang, C. Microwave-assisted Synthesis of Hierarchical Mesoporous Nano-TiO_2/Cellulose Composites for Rapid Adsorption of Pb^{2+}. *J. Chem. Eng.* **2017**, *313*, 1132-1141.
(62) Shaheen, T. I.; Salem, S. S.; Zaghloul, S. A New Facile Strategy for Multifunctional Textiles Development through In Situ Deposition of SiO_2/TiO_2 Nanosols Hybrid. *Ind. Eng. Chem. Res.* **2019**, *58* (44), 20203-20212.
(63) Tanaka, A.; Sakaguchi, S.; Hashimoto, K.; Kominami, H. Preparation of Au/TiO_2 with Metal Cocatalysts Exhibiting Strong Surface Plasmon Resonance Effective for Photoinduced Hydrogen Formation under Irradiation of Visible Light. *ACS Catal.* **2013**, *3* (1), 79-85.

(64) Su, F.; Wang, T.; Lv, R.; Zhang, J.; Zhang, P.; Lu, J.; Gong, J. Dendritic Au/TiO_2 Nanorod Arrays for Visible-Light Driven Photoelectrochemical Water Splitting. *Nanoscale* **2013**, *5* (19), 9001-9009.
(65) Li, X.; Li, C.; Xu, Y.; Liu, Q.; Bahri, M.; Zhang, L.; Browning, N. D.; Cowan, A. J.; Tang, J. Efficient Hole Abstraction for Highly Selective Oxidative Coupling of Methane by Au-sputtered TiO_2 Photocatalysts. *Nat Energy* **2023**, *8* (9), 1013-1022.
(66) Li, X. Z.; Li, F. B. Study of Au/Au^{3+}-TiO_2 Photocatalysts Toward Vsible Photooxidation for Water and Wastewater Treatment. *Environ. Sci. Technol.* **2001**, *35* (11), 2381-2387.
(67) Bhullar, V.; Devi, D.; Singh, F.; Chopra, S.; Debnath, A. K.; Aswal, D. K.; Mahajan, A. Ion Implanted Substitutionally Dispersed Au in TiO_2 Nanostructures for Efficient and Stable Dye Sensitized Solar Cells. *Opt. Mater.* **2022**, *132*, 112800.
(68) Li, F. B.; Li, X. Z. Photocatalytic Properties of Gold/Gold Ion-Modified Titanium Dioxide for Wastewater Treatment. *Appl. Catal., A* **2002**, *228* (1–2), 15-27.
(69) Matějová, L.; Kočí, K.; Reli, M.; Čapek, L.; Matějka, V.; Šolcová, O.; Obalová, L. On Sol–Gel Derived Au-Enriched TiO_2 and TiO_2-ZrO_2 Photocatalysts and Their Investigation in Photocatalytic Reduction of Carbon Dioxide. *Appl. Surf. Sci.* **2013**, *285*, 688-696.
(70) Shareena Dasari, T. P.; Zhang, Y.; Yu, H. Antibacterial Activity and Cytotoxicity of Gold (I) and (III) Ions and Gold Nanoparticles. *Biochem Pharmacol (Los Angel)* **2015**, *4* (6), From NLM.
(71) Zhang, Y.; Shareena Dasari, T. P.; Deng, H.; Yu, H. Antimicrobial Activity of Gold Nanoparticles and Ionic Gold. *J. Environ. Sci. Health C* **2015**, *33* (3), 286-327.
(72) Bhandari, V.; Jose, S.; Badanayak, P.; Sankaran, A.; Anandan, V. Antimicrobial Finishing of Metals, Metal Oxides, and Metal Composites on Textiles: A Systematic Review. *Ind. Eng. Chem. Res.* **2022**, *61* (1), 86-101.
(73) Pakdel, E.; Daoud, W. A.; Wang, X. Assimilating the Photo-Induced Functions of TiO_2-based Compounds in Textiles: Emphasis on the Sol-Gel Process. *Text. Res. J.* **2014**, *85* (13), 1404-1428.
(74) Yang, H.; Zhu, S.; Pan, N. Studying the Mechanisms of Titanium Dioxide as Ultraviolet-Blocking Additive for Films and Fabrics by an Improved Scheme. *J. Appl. Polym. Sci.* **2004**, *92* (5), 3201-3210.
(75) Pakdel, E.; Daoud, W. A.; Sun, L.; Wang, X. Reprint of: Photostability of Wool Fabrics Coated With Pure and Modified TiO_2 Colloids. *J. Colloid Interface Sci.* **2015**, *447*, 191-201.
(76) Wong, A.; Daoud, W. A.; Liang, H.-h.; Szeto, Y. S. Application of Rutile and Anatase onto Cotton Fabric and Their Effect on the NIR Reflection/Surface Temperature of the Fabric. *Sol. Energy Mater. Sol. Cells* **2015**, *134*, 425-437.
(77) Huang, L.; Liu, X.; Wu, H.; Wang, X.; Wu, H.; Li, R.; Shi, L.; Li, C. Surface State Modulation for Size-Controllable Photodeposition of Noble Metal Nanoparticles on Semiconductors. *J. Mater. Chem. A,* **2020**, *8* (40), 21094-21102.
(78) Veziroglu, S.; Obermann, A.-L.; Ullrich, M.; Hussain, M.; Kamp, M.; Kienle, L.; Leißner, T.; Rubahn, H.-G.; Polonskyi, O.; Strunskus, T.; et al. Photodeposition of Au Nanoclusters for Enhanced Photocatalytic Dye Degradation over TiO_2 Thin Film. *ACS Appl. Mater. Interfaces* **2020**, *12* (13), 14983-14992.
(79) Pakdel, E.; Wang, X. Thermoregulating Textiles and Fibrous Materials for Passive Radiative Cooling Functionality. *Mater. Des.* **2023**, *231*, 112006.
(80) Tung, W. S.; Daoud, W. A.; Leung, S. K. Understanding Photocatalytic Behavior on Biomaterials: Insights from TiO_2 Concentration. *J. Colloid Interface Sci.* **2009**, *339* (2), 424-433.

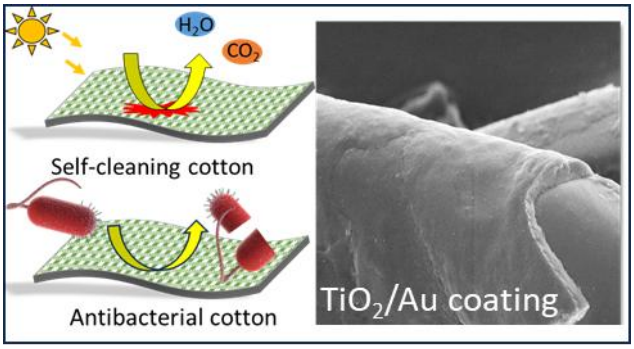

Abstract Graphic